Contribution from the Department of Chemistry,
Colorado State University, Fort Collins, Colorado 80523

Highly Polydentate Ligands. 5.[1] Structures of Alkaline-Earth Complexes of the Calcium-Selective Ligand $EGTA^{4-}$ (H_4EGTA = 3,12-Bis(carboxymethyl)-6,9-dioxa-3,12-diazatetradecanedioic Acid)

Cynthia K. Schauer and Oren P. Anderson*

Received May 10, 1988

The structures of salts of the magnesium, calcium, strontium, and barium complexes of the octadentate ligand $EGTA^{4-}$ have been investigated by single-crystal X-ray diffraction, in order to determine the ways in which this highly calcium-selective ligand coordinates the alkaline-earth metal ions. Compound **1**, $Sr[Ca(EGTA)]\cdot 6H_2O$, crystallizes in the triclinic space group $P\bar{1}$ (Z = 2), with a = 8.410 (1) Å, b = 11.282 (2) Å, c = 13.833 (2) Å, α = 88.60 (1)°, β = 73.88 (1)°, and γ = 78.45 (1)°. Compound **2**, $Mg[Sr(EGTA)(OH_2)]\cdot 7H_2O$, crystallizes in the orthorhombic space group $Pccn$ (Z = 8), with a = 21.331 (4) Å, b = 16.799 (4) Å, and c = 14.372 (2) Å. Compound **3**, $Mg[Ba(EGTA)]\cdot {}^{8}/_{3}H_2O\cdot {}^{1}/_{3}(CH_3)_2CO$, crystallizes in the orthorhombic space group $Pca2_1$ (Z = 12), with a = 21.801 (5) Å, b = 15.444 (2) Å, and c = 20.115 (4) Å. Compound **4**, $[Mg_2(EGTA)(OH_2)_6]\cdot 5H_2O$, crystallizes in the orthorhombic space group $Pna2_1$ (Z = 4), with a = 14.098 (2) Å, b = 12.396 (3) Å, and c = 15.925 (3) Å. In **1**, Ca^{2+} and $EGTA^{4-}$ form an octadentate chelate; the $[Ca(EGTA)]^{2-}$ complex anion exhibits a distorted dodecahedral coordination sphere. The nitrogen atoms bind to Ca^{2+} at longer distances (Ca–N(av) = 2.592 (9) Å) than do the ether oxygen atoms (Ca–O(ether)(av) = 2.51 (2) Å) or the carboxylate oxygen atoms (Ca–O(carboxylate)(av) = 2.377 (8) Å). In **2**, a water molecule occupies a coordination site in the nine-coordinate $[Sr(EGTA)(OH_2)]^{2-}$ complex. The aqua ligand forms the shortest bond to Sr^{2+} (Sr–w1 = 2.554 (5) Å), and the nitrogen atoms of $EGTA^{4-}$ form the longest bonds (Sr–N(av) = 2.85 (6) Å). The Sr–O(carboxylate) and the Sr–O(ether) bond distances are similar in length (Sr–O(carboxylate)(av) = 2.67 (6) Å, Sr–O(ether)(av) = 2.63 (3) Å); the Sr–O(carboxylate) distances, in particular, cover a considerable range (2.588 (4)–2.722 (5) Å). In **3**, three formula units occupy the crystallographic asymmetric unit, and 10-coordination about Ba^{2+} in the Ba^{2+}–$EGTA^{4-}$ complex is achieved by coordination of two carboxylate oxygen atoms from adjacent complex anions. Ba–O(ether) distances are similar to Ba–O(carboxylate) distances (Ba–O(ether)(av) = 2.84 (6) Å, Ba–O(carboxylate)(av) = 2.81 (3) Å); Ba–N distances (Ba–N(av) = 2.89 (3) Å) are longer than Ba–O distances. In the dinuclear compound **4**, each end of the $EGTA^{4-}$ ligand acts as a tridentate ligand, using an amino nitrogen atom and two carboxylate oxygen atoms to bind at three corners of a single face of an octahedral Mg^{2+} ion. The remaining three coordination sites on each Mg^{2+} are occupied by water molecules. The water molecules and the carboxylate oxygen atoms form bonds to Mg^{2+} that are equivalent in length (Mg–O(carboxylate)(av) = 2.07 (2) Å, Mg–O(water)(av) = 2.05 (3) Å), while the amine nitrogen atoms are bound at longer distances (Mg–N(av) = 2.30 (3) Å). Comparison of the structures of these alkaline-earth complexes suggests reasons for the calcium-binding selectivity exhibited by $EGTA^{4-}$.

Introduction

The ability of calcium-binding proteins to sequester calcium ion preferentially over magnesium ion is immensely important in biological regulatory processes.[2] The potentially octadentate ligand $EGTA^{4-}$ (H_4EGTA = 3,12-bis(carboxymethyl)-6,9-dioxa-3,12-diazatetradecanedioic acid) exhibits a strong preference for binding calcium ion over magnesium ion (see Table I); as a result, $EGTA^{4-}$ has been used extensively as a calcium buffer in biological studies.[7] The calcium-binding selectivity exhibited by $EGTA^{4-}$ ($K([Ca(EGTA)]^{2-}) \approx 10^6 K([Mg(EGTA)]^{2-})$) is even greater than the selectivity for Ca^{2+} exhibited by the calcium-binding proteins. $EGTA^{4-}$ and the calcium-binding proteins[8] also bind calcium preferentially over strontium and barium; $[Sr(EGTA)]^{2-}$ and $[Ba(EGTA)]^{2-}$ exhibit stability constants that are almost 3 orders of magnitude lower than that for the $[Ca(EGTA)]^{2-}$ complex. The common hexadentate ligand $EDTA^{4-}$ (H_4EDTA = 3,6-bis(carboxymethyl)-3,6-diazaoctanedioic acid), is also capable of calcium-selective binding, but the selectivity for binding Ca^{2+} over Mg^{2+} is much smaller for $EDTA^{4-}$ than for $EGTA^{4-}$.

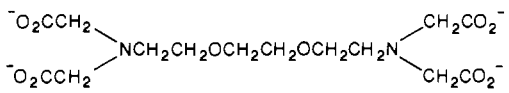

$EGTA^{4-}$

Table I. Selected Stability Constants

ligand	log K				ref
	Mg^{2+}	Ca^{2+}	Sr^{2+}	Ba^{2+}	
calmodulin	3.0	6.0–7.2			3, 4
$EDTA^{4-}$	8.8	10.7	8.7	7.9	5
$EGTA^{4-}$	5.2	11.0	8.5	8.4	5
$BAPTA^{4-}$	1.8	7.0			6

This report presents structural results for magnesium, calcium, strontium, and barium complexes of $EGTA^{4-}$. The relative enthalpic and entropic contributions to the stability constants for $[M(EGTA)]^{2-}$ complexes (M^{2+} = Mg^{2+}, Ca^{2+}, Sr^{2+}, Ba^{2+}) have been determined,[9-11] but interpretation of such thermodynamic data in the absence of knowledge of the chelates' structures is difficult. This is especially true for the magnesium ion, since the preference of Mg^{2+} ion for six-coordination makes it unlikely that the Mg^{2+} ion would be able to utilize all of the binding sites of a ligand such as $EGTA^{4-}$. With the aid of the structural results reported herein and the reported structure of $Ca[Ca(EGTA)]\cdot {}^{22}/_{3}H_2O$,[12] previous interpretations of the thermodynamic results for the $EGTA^{4-}$ chelates of the alkaline-earth metal ions can be reevaluated, and an understanding of the structural features (ligand atom preferences, coordination number preferences, and

(1) Part 4: Schauer, C. K.; Anderson, O. P. *J. Chem. Soc., Dalton Trans.*, in press.
(2) (a) *Calcium in Biology*; Spiro, T. G., Ed.; Wiley: New York, 1983. (b) *Calcium and Its Role in Biology*; Sigel, H., Ed.; Marcel Dekker: New York, 1984. (c) *Calcium and Cell Function*; Cheung, W. Y., Ed.; Academic: New York, 1980; Vol. 1. *Ibid.* Academic: New York, 1982; Vol. 2. (d) Campbell, A. K. *Intracellular Calcium*; Wiley: New York, 1983. (e) *Calcium Binding Proteins*; DeBernard, B., Sottocasa, G. L., Sandri, G., Carafoli, E., Taylor, A. N., Vanaman, T. C., Williams, R. J. P., Eds.; Elsevier: New York, 1983. (f) *Calcium Binding Proteins: Structure and Function*; Siegel, F. L., Carafoli, E., Kretsinger, R. H., Mackennan, D. H., Waserman, R. H., Eds.; Elsevier North-Holland: New York, 1980. (g) Kretsinger, R. H. *CRC Crit. Rev. Biochem.* **1980**, 119. (h) *Calmodulin and Cell Function*; Waterson, D. M., Vincenzi, F. F., Eds.; New York Academy of Science: New York, 1980. (i) Means, A. R.; Tash, J. R.; Chafouleas, J. G. *Physiol. Rev.* **1982**, *62*, 1.
(3) Klee, C. B.; Vanaman, T. C. *Adv. Protein Chem.* **1982**, *35*, 213.
(4) Haiech, J.; Klee, C. B.; Demaille, J. G. *Biochemistry* **1981**, *20*, 3890.
(5) Martell, A. E.; Smith, R. M. *Critical Stability Constants*; Plenum: New York, 1974; Vol. I.
(6) Tsien, R. Y. *Biochemistry* **1980**, *19*, 2396.
(7) Reference 2d, Chapter 2.
(8) Seamon, K. B.; Kretsinger, R. H. In ref 2a, Chapter 1, p 20.
(9) Nancollas, G. H. *Coord. Chem. Rev.* **1970**, *5*, 379.
(10) Wright, D. L.; Holloway, J. H.; Reilley, C. N. *Anal. Chem.* **1965**, *37*, 884.
(11) Anderegg, G. *Helv. Chim. Acta* **1964**, *47*, 1801.
(12) Schauer, C. K.; Anderson, O. P. *J. Am. Chem. Soc.* **1987**, *109*, 3646.

0020-1669/88/1327-3118$01.50/0

Table II. Crystallographic Experiments and Computations

	1	2	3	4
formula	$C_{14}H_{20}CaN_2O_{10}Sr\cdot 6H_2O$	$C_{14}H_{20}MgN_2O_{10}Sr\cdot 8H_2O$	$C_{14}H_{20}BaMgN_2O_{10}\cdot {}^8/_3H_2O\cdot {}^1/_3(CH_3)_2CO$	$C_{14}H_{20}Mg_2N_2O_{10}\cdot 11H_2O$
formula wt	612.1	632.4	605.35	623.10
temp, °C	20 (1)	20 (1)	−130 (1)	20 (1)
cryst syst	triclinic	orthorhombic	orthorhombic	orthorhombic
space group	$P\bar{1}$	*Pccn*	$Pca2_1$	$Pna2_1$
a, Å	8.410 (1)	21.331 (4)	21.801 (5)	14.098 (2)
b, Å	11.282 (2)	16.799 (4)	15.444 (2)	12.396 (3)
c, Å	13.833 (2)	14.372 (2)	20.115 (4)	15.925 (3)
α, deg	88.60 (1)	90	90	90
β, deg	73.88 (1)	90	90	90
γ, deg	78.45 (1)	90	90	90
V, Å^3	1234.6 (3)	5150 (1)	6772 (1)	2783.2 (5)
Z	2	8	12	4
F(000)	632	2624	3640	1328
D(calcd), g cm^{-3}	1.65	1.63	1.78	1.49
cryst dimens, mm	0.48 (100 → $\bar{1}$00) × 0.18 (001 → 00$\bar{1}$) × 0.22 (010 → 0$\bar{1}$0)	0.40 (100 → $\bar{1}$00) × 0.14 (011 → 0$\bar{1}\bar{1}$) × 0.20 (122 → $\bar{1}\bar{2}\bar{2}$)	0.50 × 0.38 × 0.35	0.24 (100 → $\bar{1}$00) × 0.46 (010 → 0$\bar{1}$0) × 0.22 (001 → 00$\bar{1}$)
radiation	Mo Kα (λ = 0.7107 Å)	Mo Kα	Mo Kα	Mo Kα
monochromator	graphite	graphite	graphite	graphite
μ, cm^{-1}	25.5	22.9	19.0	1.7
scan type	$\theta/2\theta$	$\theta/2\theta$	$\theta/2\theta$	$\theta/2\theta$
2θ range, deg	3.5–50	3.5–50	3.5–50	3.5–58
indices	$\pm h,\pm k,+l$	$+h,-k,-l$	$-h,+k,\pm l$	$-h,+k,-l$
no. of reflns	4087 measd, 3888 unique, 3152 used ($I > 2\sigma(I)$)	5086 measd, 4571 unique, 2832 used ($I > 2\sigma(I)$)	17 756 measd, 8478 unique, 7845 used ($I > 2.5\sigma(I)$)	4168 measd, 3846 unique, 2914 used ($I > 2.5\sigma(I)$)
scan speed, deg min^{-1}	variable, 2–29	variable, 2–29	variable, 5–29	variable, 2–29
no. of least-squares params	307	327	872	371
data/param	10.3	8.7	9.3	7.9
R^a	0.040	0.053	0.023	0.055
$R_w{}^a$	0.049	0.060	0.030	0.073
GOF^a	1.55	1.61	0.99	1.65
g(refined)^a	4.6×10^{-4}	4.2×10^{-4}	4.6×10^{-4}	1.0×10^{-4} (fixed)
slope, normal prob plot^b	1.19	1.18	0.85	1.30

$^a R = (\sum|F_o - F_c|)/(\sum F_o)$; $R_w = \{(\sum w(F_o - F_c)^2)/(\sum w(F_o)^2)\}^{1/2}$, $w = (\sigma^2(F) + gF^2)^{-1}$; GOF = $\{(\sum w(F_o - F_c)^2)/(N_{data} - N_{params})\}^{1/2}$. ^{b}Abrahams, S. C. *Acta Crystallogr., Sect. B: Struct. Crystallogr. Cryst. Chem.* **1974**, *B30*, 261.

steric constraints) associated with the calcium-binding selectivity of $EGTA^{4-}$ may be achieved.

The calcium-binding domains of calcium-binding proteins are likely to include four carboxylate donors, together with several other types of neutral oxygen donors. These domains can thus sequester the Ca^{2+} ion in an "all oxygen" coordination environment. The two amine nitrogen donors of $EGTA^{4-}$ prevent it from being regarded as a faithful "model" for the binding sites of calcium-binding proteins. Many features of this ligand (the 4– charge on the binding site, the presence of four carboxylate moieties, and the mixture of neutral and anionic oxygen donors) make it an interesting model, however, and an understanding of the structural aspects of alkaline-earth binding that are associated with the high degree of calcium selectivity seen for $EGTA^{4-}$ may allow a better understanding of the features that are likely to be employed in the binding sites of calcium-binding proteins.

Experimental Section

All chemicals were used as purchased (H_4EGTA (J. T. Baker), $Ca(OH)_2$ (Fisher), $Sr(OH)_2\cdot 8H_2O$ (Alfa), $Ba(OH)_2\cdot 8H_2O$ (MCB), and $Mg(OH)_2$ (Alfa)).

Preparations. Sr[Ca(EGTA)]·6H$_2$O (1). $Ca(OH)_2$(s) (0.074 g, 1.00 mmol) and $Sr(OH)_2\cdot 8H_2O$(s) (0.265 g, 1.00 mmol) were added to an aqueous slurry (15 mL) of H_4EGTA (0.380 g, 1.00 mmol). The solids dissolved on warming and stirring. The pH was adjusted to 8 by adding $Ca(OH)_2$(s). The volume of the warm solution was reduced to 10 mL by evaporation, and a 25-mL aliquot of acetone was then added. Slow cooling of the solution to room temperature yielded colorless crystals suitable for X-ray diffraction studies. The ^{1}H NMR spectrum of a solution of **1** in D_2O was identical with that of $Ca[Ca(EGTA)]\cdot {}^{22}/_3H_2O$.[12]

Mg[Sr(EGTA)(OH$_2$)]·7H$_2$O (2). $Mg(OH)_2$(s) (0.058 g, 1.0 mmol) and $Sr(OH)_2\cdot 8H_2O$(s) (0.265 g, 1.00 mmol) were added to an aqueous slurry (30 mL) of H_4EGTA (0.380 g, 1.00 mmol). When the mixture was heated and stirred, a cloudy solution of neutral pH was obtained. Addition of acetone to a total volume of 75 mL induced precipitation of **2** as a powder. Single crystals of **2** suitable for X-ray diffraction experiments were grown by vapor diffusion of acetone (over a period of 2–3 weeks) into filtered 2–4-mL samples of a 0.09 M aqueous solution of **2** prepared from the isolated powder. The colorless single crystals were characterized by the X-ray structure determination and by ^{1}H NMR spectroscopy.[13]

Mg[Ba(EGTA)]·$^8/_3$H$_2$O·$^1/_3$(CH$_3$)$_2$CO (3). $Mg(OH)_2$(s) (0.058 g, 1.0 mmol) and $Ba(OH)_2\cdot 8H_2O$(s) (0.315 g, 1.00 mmol) were added to an aqueous slurry (25 mL) of H_4EGTA (0.380 g, 1.00 mmol), yielding a cloudy solution of approximately neutral pH upon stirring and heating. The volume of the solution was reduced to approximately 5 mL; cooling and addition of acetone to a total volume of 15 mL induced precipitation of **3** as a powder. Colorless single crystals of **3** suitable for X-ray diffraction studies were grown by repeated recrystallization by vapor diffusion of acetone into 2-mL aliquots of 0.08 M solutions of the barium complex. The NMR spectrum of **3** in D_2O was identical with the previously reported spectrum of the $[Ba(EGTA)]^{2-}$ complex anion.[13]

[Mg$_2$(EGTA)(OH$_2$)$_6$]·5H$_2$O (4). $Mg(OH)_2$(s) (0.116 g, 2.00 mmol) was added to an aqueous slurry (20 mL) of H_4EGTA (0.380 g, 1.00 mmol). This mixture was stirred and heated overnight, and the pH of the cooled solution was adjusted to 9 by addition of $Mg(OH)_2$(s). Colorless crystals suitable for X-ray diffraction studies were obtained on slow evaporation.

X-ray Structure Determinations. Crystal data for **1–4**, along with details of the X-ray diffraction experiments and parameters related to subsequent computations, are tabulated in Table II. All data were collected on a Nicolet R3m diffractometer.[14] Crystal stability in the beam was monitored by measuring the intensities of three control reflections at regular intervals; when necessary, the data were scaled to correct for slight degradation of the crystal during the diffraction experiment. In addition, Lorentz and polarization corrections were applied to the raw data. Absorption corrections were performed as described below. Neutral atom scattering factors with anomalous scattering con-

(13) Bryson, A.; Nancollas, G. H. *Chem. Ind. (London)* **1965**, 654.
(14) Software used for diffractometer operations and data collection was provided with the Nicolet R3m diffractometer. Crystallographic computations were carried out with the SHELXTL program library, written by G. M. Sheldrick and supplied by Nicolet Corp., XRD Division.

Table III. Atomic Coordinates (Fractional, $\times 10^4$) and Equivalent Isotropic Thermal Parameters ($Å^2 \times 10^3$) for $Sr[Ca(EGTA)]\cdot 6H_2O$ (**1**)[a]

atom	x	y	z	U_{iso}[b]
Ca	7601 (1)	2627 (1)	−2603 (1)	23 (1)
Sr	10989 (1)	5069 (1)	−1597 (1)	33 (1)
C1	5947 (5)	1780 (4)	−4335 (3)	32 (2)
C2	6119 (5)	717 (3)	−3645 (3)	29 (2)
C3	6815 (6)	3710 (4)	−4794 (4)	36 (2)
C4	7238 (5)	4717 (4)	−4261 (3)	30 (2)
C5	8899 (5)	1834 (4)	−5022 (3)	32 (2)
C6	10381 (5)	2285 (4)	−4864 (3)	37 (2)
C7	11435 (6)	955 (4)	−3695 (4)	41 (2)
C8	11392 (5)	874 (4)	−2609 (4)	39 (2)
C9	9439 (6)	892 (4)	−1007 (4)	41 (2)
C10	7580 (5)	980 (4)	−511 (4)	36 (2)
C11	4790 (5)	1992 (4)	−578 (4)	33 (2)
C12	3864 (5)	2901 (4)	−1171 (3)	32 (2)
C13	6632 (5)	3159 (4)	−143 (3)	34 (2)
C14	8030 (5)	3826 (4)	−633 (3)	28 (2)
N1	7266 (4)	2499 (3)	−4408 (3)	27 (1)
N2	6544 (4)	2118 (3)	−730 (3)	27 (1)
O1	6863 (4)	791 (3)	−2984 (2)	40 (1)
O2	5469 (4)	−137 (3)	−3777 (3)	45 (1)
O3	7590 (4)	4494 (3)	−3438 (2)	40 (1)
O4	7145 (4)	5721 (3)	−4659 (2)	40 (1)
O5	10450 (4)	2111 (2)	−3838 (2)	33 (1)
O6	9670 (4)	989 (3)	−2056 (2)	34 (1)
O7	4705 (4)	3462 (3)	−1844 (3)	42 (1)
O8	2279 (4)	3011 (3)	−941 (2)	42 (1)
O9	8704 (4)	3689 (3)	−1569 (2)	33 (1)
O10	8432 (4)	4524 (3)	−95 (2)	40 (1)
w1[c]	9298 (5)	6089 (3)	−2821 (3)	67 (2)
w2	9587 (4)	7343 (3)	−983 (3)	52 (1)
w3	13622 (4)	5875 (3)	−2418 (3)	56 (2)
w4	12080 (4)	3885 (3)	−3317 (2)	45 (1)
w5	14478 (5)	2424 (3)	3204 (3)	57 (2)
w6	12599 (6)	1425 (3)	2121 (3)	78 (2)

[a] Estimated standard deviations in the least significant digits are given in parentheses. [b] The equivalent isotropic U is equal to one-third of the trace of the U_{ij} tensor. [c] w*n* designates the oxygen atom of the *n*th water molecule.

tributions were utilized in the computations.[15] Hydrogen atoms of the $EGTA^{4-}$ ligands were included by placement in idealized positions (C–H = 0.96 Å, $U(H) = 1.2U_{iso}(C)$).

$Sr[Ca(EGTA)]\cdot 6H_2O$ (1). The cell dimensions reported for **1** were obtained from a least-squares fit of the cell constants to the setting angles for 25 reflections ($2\theta(av) = 21.98°$). The intensities of three control reflections ($\bar{1}\bar{1}4$, $\bar{3}10$, 030), measured every 97 reflections, showed no significant trend over the course of data collection. An empirical absorption correction was applied to the raw data, with use of the intensity profiles for 15 reflections as a function of ψ ($\Delta\psi = 15°$). The range of transmission factors exhibited for the complete data set was ±8% of the mean value.

The structure was solved by the direct-methods routine SOLV. The initial E map clearly revealed the positions of the Sr^{2+} and Ca^{2+} ions. Subsequent Fourier difference maps revealed the positions of all non-hydrogen atoms of the $EGTA^{4-}$ ligand and the oxygen atoms of six water molecules (four of which were bound to Sr^{2+}). In the final structural model, all non-hydrogen atoms were given anisotropic thermal parameters. At convergence ($(shift/esd)_{av} < 0.02$ over the last three cycles), the highest peaks in the difference electron density map corresponded to hydrogen atoms of water molecules (0.5 e $Å^{-3}$); the minimum in the map was −0.4 e $Å^{-3}$.

Final fractional atomic coordinates for all non-hydrogen atoms of **1** may be found in Table III. Metric parameters that describe the coordination of the Sr^{2+} and Ca^{2+} ions and the interaction between these species may be found in Table IV. Ligand structural parameters (Table V) have also been tabulated.

$Mg[Sr(EGTA)(OH_2)]\cdot 7H_2O$ (2). The cell dimensions reported for **2** were obtained from a least-squares fit of the cell constants to the setting angles for 25 reflections ($2\theta(av) = 17.33°$). The intensities of three standard reflections ($00\bar{8}$, 800, and $0\bar{8}0$), measured every 97 reflections, declined by an average of 6% during data collection; the data were

(15) *International Tables for X-Ray Crystallography*; Kynoch: Birmingham, England, 1974; Vol. IV, pp 99, 149.

Table IV. Metal–Ligand Distances (Å) and Angles (deg)[a] for $Sr[Ca(EGTA)]\cdot 6H_2O$ (**1**)

	a. Complex Ion		
Ca–N1	2.599 (4)	Ca–N2	2.586 (3)
Ca–O1	2.387 (3)	Ca–O3	2.377 (3)
Ca–O5	2.493 (3)	Ca–O6	2.528 (3)
Ca–O7	2.373 (3)	Ca–O9	2.369 (4)
N1–Ca–N2	147.0 (1)	N1–Ca–O1	66.0 (1)
N2–Ca–O1	86.5 (1)	N1–Ca–O3	66.8 (1)
N2–Ca–O3	132.3 (1)	O1–Ca–O3	131.7 (1)
N1–Ca–O5	70.6 (1)	N2–Ca–O5	131.3 (1)
O1–Ca–O5	92.5 (1)	O3–Ca–O5	81.3 (1)
N1–Ca–O6	119.3 (1)	N2–Ca–O6	67.1 (1)
O1–Ca–O6	76.0 (1)	O3–Ca–O6	138.7 (1)
O5–Ca–O6	65.5 (1)	N1–Ca–O7	94.7 (1)
N2–Ca–O7	66.0 (1)	O1–Ca–O7	89.9 (1)
O3–Ca–O7	84.2 (1)	O5–Ca–O7	162.5 (1)
O6–Ca–O7	131.7 (1)	N1–Ca–O9	143.3 (1)
N2–Ca–O9	68.5 (1)	O1–Ca–O9	148.3 (1)
O3–Ca–O9	79.9 (1)	O5–Ca–O9	90.1 (1)
O6–Ca–O9	76.5 (1)	O7–Ca–O9	96.9 (1)
	b. Counterion		
Sr–O9	2.697 (3)	Sr–O10	2.703 (3)
Sr–w1	2.608 (5)	Sr–w2	2.653 (3)
Sr–w3	2.526 (3)	Sr–w4	2.595 (3)
$Sr–O7_a$	3.215 (3)	$Sr–O8_a$	2.613 (3)
$Sr–O10_a$	2.588 (4)		
O9–Sr–O10	48.1 (1)	O9–Sr–w1	74.9 (1)
O10–Sr–w1	99.9 (1)	O9–Sr–w2	113.1 (1)
O10–Sr–w2	84.4 (1)	w1–Sr–w2	70.4 (1)
O9–Sr–w3	153.3 (1)	O10–Sr–w3	157.9 (1)
w1–Sr–w3	95.1 (1)	w2–Sr–w3	85.5 (1)
O9–Sr–w4	74.9 (1)	O10–Sr–w4	122.0 (1)
w1–Sr–w4	70.4 (1)	w2–Sr–w4	135.7 (1)
w3–Sr–w4	78.4 (1)	$O9–Sr–O7_a$	112.0 (1)
$O10–Sr–O7_a$	117.4 (1)	$w1–Sr–O7_a$	135.6 (1)
$w2–Sr–O7_a$	132.9 (1)	$w3–Sr–O7_a$	58.3 (1)
$w4–Sr–O7_a$	69.7 (1)	$O9–Sr–O8_a$	76.8 (1)
$O10–Sr–O8_a$	75.2 (1)	$w1–Sr–O8_a$	145.1 (1)
$w2–Sr–O8_a$	141.1 (1)	$w3–Sr–O8_a$	101.1 (1)
$w4–Sr–O8_a$	82.9 (1)	$O7_a–Sr–O8_a$	43.4 (1)
$O9–Sr–O10_a$	117.5 (1)	$O10–Sr–O10_a$	72.1 (1)
$w1–Sr–O10_a$	141.1 (1)	$w2–Sr–O10_a$	71.0 (1)
$w3–Sr–O10_a$	86.0 (1)	$w4–Sr–O10_a$	146.6 (1)
$O7_a–Sr–O10_a$	77.0 (1)	$O8_a–Sr–O10_a$	71.3 (1)
	c. Interionic Angles		
$Ca–O7–Sr_a$	158.2 (1)	$C12–O7–Sr_a$	80.2 (2)
$C12–O8–Sr_a$	108.6 (3)	Ca–O9–Sr	143.7 (1)
Sr–O9–C14	94.6 (3)	Sr–O10–C14	94.5 (2)
$Sr–O10–Sr_b$	107.9 (1)	$C14–O10–Sr_b$	148.2 (3)

[a] Estimated standard deviations in the least significant digits are given in parentheses.

corrected for this decrease. An empirical absorption correction was applied to the raw data, with use of the intensity profiles for nine reflections as a function of ψ ($\Delta\psi = 15°$). The range of transmission factors exhibited for the complete data set was ±20% of the mean value.

The space group was determined to be *Pnaa* by the systematic absences. Conversion to the standard space group (see Table II) was carried out by using the matrix $(001/0\bar{1}0/100)$. The Sr^{2+} ion was placed in a general position after analysis of the Patterson map. The two highest peaks in the subsequent difference Fourier electron density map appeared on the special positions (0, 0, $^1/_2$) and ($^1/_4$, $^1/_4$, z) of $\bar{1}$ and 2 symmetry, respectively. These peaks were identified as the Mg^{2+} counterions (each with a site occupancy factor of 0.5, giving a total of one Mg^{2+} counterion for each $[Sr(EGTA)]^{2-}$ unit). All non-hydrogen atoms of the $EGTA^{4-}$ ligand, together with the oxygen atoms of eight water molecules (one bound to Sr^{2+}, one bound to each Mg^{2+}, five occluded) were revealed in subsequent difference electron density maps. In the final structural model, all non-hydrogen atoms were given anisotropic thermal parameters. At convergence ($(shift/esd)_{av} < 0.01$ over the last three cycles), the highest peaks in the difference electron density map corresponded to hydrogen atoms of water molecules (0.6 e $Å^{-3}$); the minimum in the map was −0.6 e $Å^{-3}$.

Final fractional atomic coordinates for all non-hydrogen atoms of **2** may be found in Table VI. Metric parameters that describe the coor-

Table V. Chelate Ring[a] Bonding Parameters[b] for Sr[Ca(EGTA)]·6H_2O (**1**)

Glycinate Rings

	C–C′	C′–N	C–O	C–O′	C–C′–N	O–C–O′	C′–C–O	C′–C–O′	Ca–N–C′	Ca–O–C
G1	1.524 (6)	1.481 (6)	1.256 (6)	1.239 (6)	111.8 (4)	125.9 (4)	117.8 (4)	116.3 (4)	106.1 (2)	122.5 (3)
G2	1.519 (7)	1.471 (5)	1.261 (6)	1.246 (5)	114.2 (4)	124.9 (4)	118.3 (4)	116.8 (4)	111.5 (3)	125.8 (3)
G3	1.524 (6)	1.467 (6)	1.245 (5)	1.262 (5)	112.3 (3)	125.1 (4)	118.7 (4)	116.2 (4)	105.4 (3)	119.4 (3)
G4	1.515 (6)	1.470 (6)	1.259 (5)	1.251 (6)	115.4 (3)	122.5 (4)	119.1 (4)	118.4 (4)	106.2 (2)	121.4 (3)

Amino–Ether Rings

	C–C′	C–N	C′–O	C–C′–O	C′–C–N	C″–N–C†	C–N–C″	C–N–C†	Ca–N–C	Ca–O–C′
A1	1.507 (7)	1.464 (5)	1.444 (6)	110.2 (3)	113.3 (4)	112.0 (4)	110.0 (3)	111.6 (3)	105.4 (3)	112.3 (2)
A2	1.507 (6)	1.476 (5)	1.414 (6)	107.9 (4)	112.4 (4)	111.2 (3)	110.7 (3)	112.4 (4)	110.6 (2)	116.4 (2)

Diether Rings

	C–C′	C′–O′	C–O	C′–C–O	C–C′–O′	C′–O′–C†	C″–O–C	Ca–O–C	Ca–O′–C′
E1	1.493 (7)	1.419 (5)	1.439 (5)	108.3 (3)	106.7 (4)	112.9 (4)	113.2 (3)	114.3 (2)	115.2 (3)

[a] Chelate ring designations have been assigned systematically, as follows. Within each series, rings are numbered according to increasing oxygen atom number. For glycinate rings, C′ is adjacent to N, and O′ is the carboxylate oxygen atom not bound to the metal in the EGTA chelate. Within amino–ether rings, C′ is adjacent to O and C is adjacent to N; C″ and C† are also attached to N, with C″ possessing the lower number of these two atoms. Within diether rings, C′ is bound to O′ (always odd numbered), and C is bound to O; C″ is also bound to O, and C† is bound to O′. [b] Bond lengths are given in angstroms and bond angles in degrees. Estimated standard deviations in the least significant digits are given in parentheses.

Table VI. Atomic Coordinates (Fractional, ×10^4) and Equivalent Isotropic Thermal Parameters (Å^2 × 10^3) for Mg[Sr(EGTA)(OH_2)]·7H_2O (**2**)[a]

atom	*x*	*y*	*z*	U_{iso}[b]
Sr	1166 (1)	1149 (1)	3892 (1)	26 (1)
Mg1	0	0	5000	29 (1)
Mg2	2500	2500	3010 (2)	29 (1)
C1	−30 (3)	2548 (4)	4655 (5)	36 (2)
C2	−156 (3)	1758 (4)	5116 (5)	30 (2)
C3	602 (3)	3215 (4)	3501 (5)	38 (3)
C4	1190 (3)	3110 (4)	2928 (5)	34 (2)
C5	−150 (3)	2199 (4)	3055 (5)	41 (3)
C6	151 (4)	1932 (4)	2164 (5)	40 (3)
C7	835 (4)	954 (4)	1523 (5)	43 (3)
C8	1128 (4)	185 (4)	1724 (5)	42 (3)
C9	1940 (4)	−421 (4)	2620 (5)	45 (3)
C10	2401 (3)	−229 (4)	3374 (5)	38 (3)
C11	1853 (3)	−706 (4)	4747 (5)	36 (3)
C12	1348 (3)	−516 (4)	5448 (5)	32 (2)
C13	2533 (4)	426 (4)	4865 (5)	37 (2)
C14	2672 (3)	1289 (4)	4599 (5)	32 (2)
N1	295 (2)	2464 (3)	3772 (3)	28 (2)
N2	2090 (3)	4 (3)	4255 (4)	32 (2)
O1	99 (2)	1151 (3)	4750 (3)	32 (1)
O2	−484 (2)	1736 (3)	5842 (3)	44 (2)
O3	1520 (2)	2509 (3)	3052 (3)	32 (2)
O4	1318 (2)	3666 (3)	2369 (4)	55 (2)
O5	527 (2)	1244 (3)	2352 (3)	35 (2)
O6	1566 (2)	286 (3)	2464 (3)	38 (2)
O7	968 (2)	38 (3)	5238 (3)	35 (2)
O8	1319 (2)	−932 (3)	6167 (4)	45 (2)
O9	2384 (2)	1569 (3)	3908 (3)	31 (1)
O10	3055 (3)	1634 (3)	5096 (4)	60 (2)
w1	1388 (2)	1936 (3)	5377 (4)	46 (2)
w2	285 (2)	−199 (3)	3608 (3)	33 (2)
w3	2475 (3)	1644 (3)	1958 (3)	43 (2)
w4	1543 (4)	7383 (5)	3559 (5)	113 (4)
w5	708 (2)	5091 (3)	2554 (4)	46 (2)
w6	580 (3)	5323 (4)	4565 (4)	84 (3)
w7	1846 (3)	7420 (4)	1603 (4)	70 (2)
w8	1548 (3)	8552 (4)	143 (5)	91 (3)

[a] Estimated standard deviations in the least significant digits are given in parentheses. [b] The equivalent isotropic *U* is equal to one-third of the trace of the U_{ij} tensor.

dination of the Sr^{2+} and Mg^{2+} ions, as well as the interactions between these ions, may be found in Table VII. Bonding parameters (Table VIII) for the $EGTA^{4-}$ ligand have also been compiled.

Mg[Ba(EGTA)]$^{8}/_{3}H_2O^{\cdot 1}/_{3}(CH_3)_2CO$ (3). The cell dimensions for **3** were obtained from a least-squares fit of the setting angles for 25 reflections (2θ(av) = 23.18°). The intensities of three standard reflections ($\bar{6}0\bar{1}$, $00\bar{1}0$, and $\bar{5}80$), measured every 297 reflections, declined by an average of 4% during data collection; correction for this decrease was carried out. An empirical absorption correction that utilized the intensity profiles for 11 reflections as a function of ψ ($\Delta\psi$ = 15°) was applied to

Table VII. Metal–Ligand Distances (Å) and Angles (deg)[a] for Mg[Sr(EGTA)(OH_2)]·7H_2O (**2**)

a. Complex Ion

Sr–N1	2.891 (5)	Sr–O6	2.654 (5)
Sr–N2	2.802 (5)	Sr–O7	2.722 (5)
Sr–O1	2.588 (4)	Sr–O9	2.691 (4)
Sr–O3	2.693 (5)	Sr–w1	2.554 (5)
Sr–O5	2.605 (4)	Sr–w2	2.970 (5)
N1–Sr–N2	170.8 (2))	O1–Sr–O9	147.6 (1)
N1–Sr–O1	57.5 (1)	O3–Sr–O9	60.7 (1)
N2–Sr–O1	122.0 (2)	O5–Sr–O9	119.7 (1)
N1–Sr–O3	60.3 (1)	O6–Sr–O9	80.8 (1)
N2–Sr–O3	118.0 (1)	O7–Sr–O9	108.9 (1)
O1–Sr–O3	117.3 (1)	N1–Sr–w1	76.9 (2)
N1–Sr–O5	64.3 (1)	N2–Sr–w1	94.0 (2)
N2–Sr–O5	124.6 (2)	O1–Sr–w1	76.4 (1)
O1–Sr–O5	86.8 (1)	O3–Sr–w1	83.3 (1)
O3–Sr–O5	73.3 (1)	O5–Sr–w1	140.8 (2)
N1–Sr–O6	125.3 (1)	O6–Sr–w1	150.4 (2)
N2–Sr–O6	62.8 (2)	O7–Sr–w1	77.9 (2)
O1–Sr–O6	130.6 (1)	O9–Sr–w1	71.3 (1)
O3–Sr–O6	91.5 (1)	N1–Sr–w2	99.6 (1)
O5–Sr–O6	62.9 (1)	N2–Sr–w2	87.0 (1)
N1–Sr–O7	117.8 (1)	O1–Sr–w2	60.7 (1)
N2–Sr–O7	60.4 (1)	O3–Sr–w2	139.7 (1)
O1–Sr–O7	61.7 (1)	O5–Sr–w2	66.4 (1)
O3–Sr–O7	160.8 (1)	O6–Sr–w2	71.4 (1)
O5–Sr–O7	124.4 (1)	O7–Sr–w2	58.4 (1)
O6–Sr–O7	103.0 (1)	O9–Sr–w2	144.3 (1)
N1–Sr–O9	114.9 (1)	w1–Sr–w2	128.8 (1)
N2–Sr–O9	60.0 (1)		

b. Counterions

counterion 1		counterion 2	
Mg1–O1	1.978 (4)	Mg2–O3	2.092 (4)
Mg1–O7	2.094 (4)	Mg2–O9	2.043 (5)
Mg1–w2	2.117 (4)	Mg2–w3	2.087 (5)
O1–Mg1–O7	84.0 (2)	O3–Mg2–O9	82.3 (2)
O1–Mg1–w2	87.2 (2)	O3–Mg2–w3	90.1 (2)
O7–Mg1–w2	82.9 (2)	O9–Mg2–w3	85.9 (2)

c. Interionic Angles

Sr–O1–Mg1	100.3 (2)	Mg1–O1–C2	131.5 (4)
Sr–O3–Mg2	106.6 (2)	Mg2–O3–C4	124.6 (4)
Sr–O7–Mg1	93.3 (2)	Mg1–O7–C12	130.2 (4)
Sr–O9–Mg2	108.2 (2)	Mg2–O9–C14	136.5 (4)
Sr–w2–Mg1	86.1 (1)		

[a] Estimated standard deviations in the least significant digits are given in parentheses.

Table VIII. Chelate Ring[a] Bonding Parameters[b] for $Mg[Sr(EGTA)(OH_2)]\cdot 7H_2O$ (**2**)

Glycinate Rings

	C–C′	C′–N	C–O	C–O′	C–C′–N	O–C–O′	C′–C–O	C′–C–O′	Sr–N–C′	Sr–O–C
G1	1.508 (9)	1.453 (9)	1.270 (8)	1.256 (9)	112.5 (6)	124.0 (6)	116.6 (6)	119.3 (6)	109.2 (4)	125.2 (4)
G2	1.512 (10)	1.474 (9)	1.242 (8)	1.262 (9)	114.4 (5)	124.7 (7)	119.1 (6)	116.1 (6)	112.6 (4)	126.5 (4)
G3	1.509 (10)	1.476 (9)	1.270 (8)	1.249 (9)	113.1 (5)	125.0 (6)	116.9 (6)	118.0 (6)	113.8 (4)	124.9 (4)
G4	1.528 (9)	1.471 (9)	1.259 (8)	1.230 (9)	115.7 (6)	127.3 (6)	117.2 (6)	115.5 (6)	103.4 (4)	112.3 (4)

Amino–Ether Rings

	C–C′	C–N	C′–O	C–C′–O	C′–C–N	C″–N–C†	C–N–C″	C–N–C†	Sr–N–C	Sr–O–C′
A1	1.501 (10)	1.471 (9)	1.433 (9)	108.7 (6)	114.3 (6)	111.1 (5)	109.5 (5)	111.1 (5)	103.0 (4)	120.2 (4)
A2	1.498 (10)	1.483 (9)	1.448 (9)	107.4 (6)	112.3 (6)	108.9 (5)	110.4 (5)	110.3 (5)	109.7 (4)	120.3 (4)

Diether Rings

	C–C′	C′–O′	C–O	C′–C–O	C–C′–O′	C′–O′–C†	C″–O–C	Sr–O–C	Sr–O′–C′
E1	1.464 (11)	1.425 (9)	1.445 (9)	109.2 (6)	108.8 (6)	112.3 (5)	111.8 (5)	116.3 (4)	115.6 (4)

[a] Chelate ring designations have been assigned systematically, as described in Table V. [b] Bond lengths are given in angstroms and bond angles in degrees. Estimated standard deviations in the least significant digits are given in parentheses.

the raw data. The range of transmission factors exhibited for the complete data set was ±5% of the mean value. Two octants of data were collected and averaged to give the final data set utilized in the crystallographic computations.

The systematic absences observed demanded that the space group be either *Pcmb* or the noncentrosymmetric alternative, $Pc2_1b$. Statistical analysis of the data gave a weak indication that $Pc2_1b$ was the correct choice ($|(E^2-1)|(av) = 0.84$ for reflections with $(\sin\theta)/\lambda = 0.15$–$0.50$). A reasonable calculated density was obtained only for $Z = 12$. A value of 12 for Z in the centrosymmetric space group would imply that one $[Ba(EGTA)]^{2-}$ complex resided on a general position and that a second such complex occupied a special position (of symmetry *m*, 2, or $\bar{1}$). No crystallographic symmetry would be imposed in the noncentrosymmetric space group, where three $[Ba(EGTA)]^{2-}$ anions would occupy general positions in the asymmetric unit.

In the Patterson synthesis, Harker line peaks at ($^1/_2$, 0, ±2*z*) were found for three unique barium ions, as expected for $Pc2_1b$. Additionally, all possible cross peaks between three barium ions were observed. Consequently, the noncentrosymmetric space group was chosen. Conversion to the standard space group, $Pca2_1$, was accomplished with the transformation matrix (001/100/010). The positions of two of the unique Ba^{2+} ions were established by analysis of the Patterson map. A subsequent difference Fourier map revealed the positions of the remaining Ba^{2+} ion and the three Mg^{2+} counterions. Repeated difference Fourier calculations established initial positions for all non-hydrogen atoms of three $EGTA^{4-}$ ligands, oxygen atoms of eight water molecules (six were bound to the three Mg^{2+} counterions, two occurred as occluded water molecules), and the carbon and oxygen atoms of a single acetone molecule. The site occupancy factor for the atoms comprising the acetone molecule was refined and was found to equal 0.90 (1). A multiplicative factor, *df*, which multiplies the imaginary components of the scattering factors ($\Delta f''$), was refined; convergence at a value of −0.93 (2) indicated that the inverted structure was correct. The final structural model utilized anisotropic thermal parameters for all non-hydrogen atoms. At convergence ($(\text{shift/esd})_{av} < 0.03$ over the last nine cycles), the highest peaks in the difference electron density map (approximately 1 e Å^{-3}) occurred very close to Ba^{2+} ions; the minimum was −0.5 e Å^{-3}.

Final fractional atomic coordinates for all non-hydrogen atoms of **3** may be found in Table IX. Metric parameters relevant to the coordination of the Ba^{2+} and Mg^{2+} ions, as well as to the interactions between these ions, may be found in Table X. Bonding parameters (Table XI) for the $EGTA^{4-}$ ligand have also been compiled.

$[Mg_2(EGTA)(H_2O)_6]\cdot 5H_2O$ (4). The cell dimensions for **4** were obtained from a least-squares refinement of the setting angles for 25 reflections ($2\theta(av) = 15.70°$). The intensities of three standard reflections (008, 303, 080) were measured every 97 reflections; these intensities showed no significant trend over the course of data collection. No absorption correction was performed, due to the small average value of μt.

The systematic absences required the space group to be either *Pbnm* or $Pbn2_1$. The structure was solved by the direct-methods routine RANT in the noncentrosymmetric space group. Transformation of the axes and indices to the standard space group, $Pna2_1$, required multiplication by the transformation matrix (010/$\bar{1}$00/001). The positions of the Mg^{2+} ions are approximately centrosymmetrically related. If *Pnam* were the correct space group choice, the halves of the dinuclear magnesium complex (see below) would be related by a mirror plane or an inversion center. In the observed structure (as solved and refined in the noncentrosymmetric space group), a single oxygen atom and the adjacent carbon atom in the diether portion of the $EGTA^{4-}$ ligand were found to be disordered. Absence of further disorder is inconsistent with the requisite *m* or $\bar{1}$ symmetry in the centrosymmetric space group. In addition, the conformation of the diether backbone is such that mirror or inversion symmetry is not possible.

The initial *E* map revealed the positions of the Mg^{2+} ions, all non-hydrogen atoms of the $EGTA^{4-}$ ligand, and the oxygen atoms of several water molecules. The final structural model utilized anisotropic thermal parameters for all non-hydrogen atoms. As mentioned above, disorder was apparent in the diether chair. The site occupancy factors for C8 (C8′) and O6 (O6′) were refined to a value of 0.75 (1) (0.25 (1)). Hydrogen atoms of the $EGTA^{4-}$ ligand were included in the model as described earlier, with the exception of this disordered portion. The parameter *df* was not refined satisfactorily (*df* = 2.2 (9), see above), which is consistent with the small degree of anomalous scattering by magnesium and the nearly centrosymmetric placement of the two Mg^{2+} ions. At convergence ($(\text{shift/esd})_{av} < 0.018$ over the last four cycles) the highest peaks (approximately 0.5 e Å^{-3}) in the difference electron density map corresponded to hydrogen atoms of water molecules; the minimum in the final difference map was −0.32 e Å^{-3}.

Final fractional atomic coordinates for all non-hydrogen atoms of **4** may be found in Table XII. Bond lengths and angles involving the Mg^{2+} ions are listed in Table XIII. Bonding parameters for the $EGTA^{4-}$ ligand may be found in Table XIV.

Results and Discussion

Structure of $Sr[Ca(EGTA)]\cdot 6H_2O$ (1). The structure of the calcium salt of $[Ca(EGTA)]^{2-}$ has been previously determined.[12] In that structure ($Ca[Ca(EGTA)]\cdot {}^{22}/_3H_2O$, hereafter **5**), partially aquated Ca^{2+} cations interacted strongly through carboxylate bridges with $[Ca(EGTA)]^{2-}$ complex anions. When single crystals of the strontium salt of $[Ca(EGTA)]^{2-}$ became available, a structure determination was undertaken to assess the effect of the change in counterion on the structure of the $[Ca(EGTA)]^{2-}$ complex anion.

The structure of **1**, with one formula unit per asymmetric unit in the solid state, is much simpler than that of **5**, in which three formula units were found in the asymmetric unit. As was the case in **5**, the partially aquated counterion in **1** interacts extensively with the $[Ca(EGTA)]^{2-}$ complex anion. These interactions, however, do not influence the arrangement of the $EGTA^{4-}$ ligand about Ca^{2+}; a thermal ellipsoid plot of the complex anion in **1** (see Figure 1) is indistinguishable from a thermal ellipsoid plot of any one of the complex anions in **5**, despite the different pattern of anion–cation bridging present in the two compounds.

In **1**, oxygen atoms from bridging carboxylate groups contribute five of the nine ligand atoms surrounding the Sr^{2+} counterion (see Figure 2). The remaining positions about Sr^{2+} are occupied by the oxygen atoms of water molecules. Two of the four carboxylate groups of the $[Ca(EGTA)]^{2-}$ anion are involved in bridging interactions. One carboxylate group (O9/O10) functions simultaneously as a bidentate and as a unidentate(O′) donor[12] to two symmetry-related Sr^{2+} ions. The other bridging carboxylate group (O7/O8) acts solely as a bidentate donor, although this bridge is quite asymmetric (Sr–O8a = 2.613 (3) Å, Sr–O7a = 3.215 (3)

Table IX. Atomic Coordinates (Fractional, $\times 10^4$) and Equivalent Isotropic Thermal Parameters ($Å^2 \times 10^3$) for $Mg[Ba(EGTA)]\cdot{}^8/_3H_2O\cdot{}^1/_3(CH_3)_2CO$ (**3**)[a]

atom	x	y	z	U_{iso}[b]	atom	x	y	z	U_{iso}[b]
Ba1	6110 (1)	8036 (1)	9189 (1)	16 (1)	C43	10551 (6)	1583 (7)	5796 (8)	115 (6)
Ba2	5066 (1)	4704 (1)	7468 (1)	16 (1)	C44	10104 (4)	1834 (5)	5284 (5)	66 (3)
Ba3	6965 (1)	1348 (1)	7398 (1)	15 (1)	C45	10369 (7)	2200 (9)	4658 (7)	107 (6)
Mg1	5439 (1)	5714 (1)	9142 (1)	17 (1)	N1	5092 (2)	8612 (2)	8406 (2)	21 (1)
Mg2	7280 (1)	9049 (1)	8025 (1)	18 (1)	N2	7057 (2)	7458 (2)	10090 (2)	22 (1)
Mg3	5440 (1)	2405 (1)	6919 (1)	17 (1)	N3	6240 (2)	5271 (2)	6917 (2)	18 (1)
C1	5238 (2)	9439 (3)	8091 (3)	24 (1)	N4	3855 (2)	4130 (2)	7928 (2)	23 (1)
C2	5897 (2)	9512 (3)	7830 (2)	18 (1)	N5	6838 (2)	1953 (2)	8744 (2)	19 (1)
C3	5031 (2)	7952 (3)	7892 (2)	24 (1)	N6	7136 (2)	769 (2)	6052 (2)	20 (1)
C4	5011 (2)	7018 (3)	8140 (2)	21 (1)	O1	6287 (1)	8952 (2)	8014 (2)	19 (1)
C5	4532 (2)	8674 (3)	8811 (3)	28 (1)	O2	6001 (1)	10157 (2)	7476 (2)	22 (1)
C6	4615 (2)	9246 (3)	9408 (3)	32 (1)	O3	5187 (1)	6882 (2)	8732 (2)	21 (1)
C7	5174 (3)	9351 (3)	10421 (3)	31 (1)	O4	4845 (2)	6467 (2)	7729 (2)	28 (1)
C8	5806 (2)	9230 (3)	10694 (2)	30 (1)	O5	5146 (2)	8979 (2)	9765 (2)	28 (1)
C9	6508 (2)	8142 (3)	11047 (2)	29 (1)	O6	5981 (2)	8329 (2)	10639 (2)	27 (1)
C10	6828 (2)	7347 (3)	10774 (2)	25 (1)	O7	7331 (1)	8339 (2)	8920 (2)	20 (1)
C11	7576 (3)	8053 (3)	10069 (2)	33 (1)	O8	8168 (2)	8947 (3)	9378 (2)	37 (1)
C12	7700 (2)	8476 (3)	9399 (2)	24 (1)	O9	6178 (1)	6309 (2)	9633 (2)	21 (1)
C13	7241 (2)	6619 (3)	9813 (2)	24 (1)	O10	6853 (2)	5233 (2)	9564 (2)	35 (1)
C14	6718 (2)	6007 (3)	9663 (2)	23 (1)	O11	5958 (1)	5576 (2)	8237 (2)	19 (1)
C15	6409 (2)	6096 (3)	7221 (2)	22 (1)	O12	6523 (1)	6795 (2)	8249 (2)	24 (1)
C16	6293 (2)	6150 (3)	7967 (2)	19 (1)	O13	5909 (1)	3560 (2)	6878 (2)	20 (1)
C17	6695 (2)	4609 (3)	7100 (2)	23 (1)	O14	6878 (1)	3110 (2)	7054 (2)	24 (1)
C18	6477 (2)	3677 (3)	6995 (2)	19 (1)	O15	5123 (2)	5461 (2)	6187 (2)	27 (1)
C19	6206 (2)	5326 (3)	6184 (2)	25 (1)	O16	4006 (2)	5036 (2)	6723 (2)	34 (1)
C20	5664 (2)	5847 (3)	5948 (2)	26 (1)	O17	4675 (1)	5041 (2)	8747 (2)	21 (1)
C21	4592 (2)	5949 (3)	6008 (3)	31 (1)	O18	3931 (2)	5327 (3)	9470 (2)	52 (2)
C22	4042 (2)	5391 (3)	6057 (3)	34 (1)	O19	4670 (1)	2971 (2)	7349 (2)	21 (1)
C23	3400 (2)	4814 (3)	6921 (3)	29 (1)	O20	4220 (2)	1859 (2)	7859 (2)	36 (1)
C24	3420 (2)	4036 (3)	7374 (3)	31 (1)	O21	5891 (1)	2219 (2)	7841 (1)	19 (1)
C25	3629 (2)	4741 (3)	8435 (3)	27 (1)	O22	5604 (2)	3448 (2)	8342 (2)	25 (1)
C26	4121 (2)	5047 (3)	8921 (2)	27 (1)	O23	7105 (1)	222 (2)	8484 (2)	20 (1)
C27	3962 (2)	3269 (3)	8225 (3)	27 (1)	O24	6528 (2)	−234 (2)	9341 (2)	24 (1)
C28	4310 (2)	2643 (3)	7766 (2)	25 (1)	O25	8002 (1)	2162 (2)	8014 (2)	28 (1)
C29	6472 (2)	2748 (2)	8785 (2)	22 (1)	O26	8047 (1)	1680 (2)	6702 (2)	28 (1)
C30	5941 (2)	2802 (2)	8287 (2)	19 (1)	O27	6122 (1)	1732 (2)	6407 (1)	18 (1)
C31	6509 (2)	1267 (3)	9094 (2)	22 (1)	O28	5992 (2)	2205 (2)	5364 (2)	27 (1)
C32	6739 (2)	334 (3)	8968 (2)	20 (1)	O29	7248 (1)	−378 (2)	7095 (2)	21 (1)
C33	7445 (2)	2085 (3)	9045 (2)	26 (1)	O30	6833 (2)	−1458 (2)	6491 (2)	34 (1)
C34	7870 (2)	2624 (3)	8617 (3)	29 (1)	O31	9572 (3)	1780 (5)	5355 (4)	86 (3)
C35	8312 (2)	2702 (3)	7549 (3)	35 (1)	w1	5761 (1)	4498 (2)	9404 (2)	21 (1)
C36	8535 (2)	2154 (4)	6981 (3)	42 (2)	w2	4948 (1)	5910 (2)	9992 (2)	25 (1)
C37	8192 (2)	1372 (3)	6044 (2)	28 (1)	w3	7325 (1)	7841 (2)	7569 (2)	25 (1)
C38	7782 (2)	599 (3)	5899 (2)	27 (1)	w4	8219 (1)	9284 (2)	8090 (2)	25 (1)
C39	6877 (2)	1397 (3)	5577 (2)	22 (1)	w5	5038 (1)	2728 (2)	5990 (2)	23 (1)
C40	6283 (2)	1809 (3)	5803 (2)	19 (1)	w6	10049 (1)	8817 (2)	7037 (2)	20 (1)
C41	6788 (2)	−42 (3)	6041 (2)	23 (1)	w7	7722 (2)	3395 (3)	5945 (2)	43 (1)
C42	6973 (2)	−676 (3)	6582 (2)	24 (1)	w8	7772 (2)	4078 (3)	9805 (2)	47 (1)

[a] Estimated standard deviations in the least significant digits are given in parentheses. [b] The equivalent isotropic U is equal to one-third of the trace of the U_{ij} tensor.

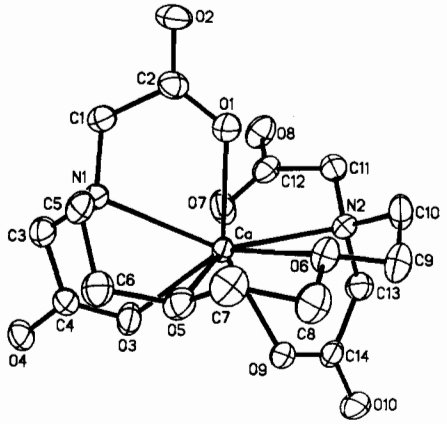

Figure 1. Thermal ellipsoid plot (50%) of the $[Ca(EGTA)]^{2-}$ complex ion in **1**.

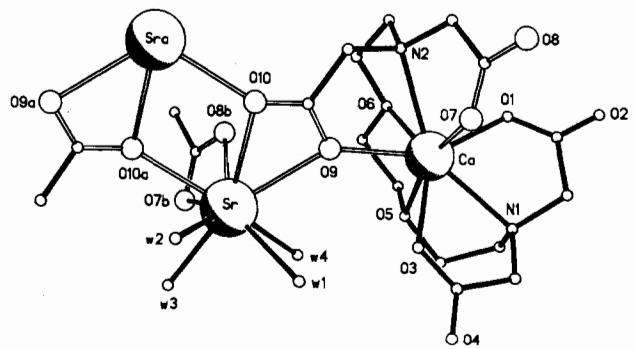

Figure 2. Ball and stick plot (arbitrary radii) depicting the interionic interactions in the solid state for **1**. Oxygen atoms that are involved in bridging interactions are enlarged. Hollowed bonds highlight the bridging pathways between the $[Ca(EGTA)]^{2-}$ anions and the Sr^{2+} counterions.

Å). The coordination about Sr^{2+} is best described by thinking of the nine ligand atoms about Sr^{2+} as occupying the vertices of a slightly twisted tricapped trigonal prism. The triangular faces of the prism are composed of two sets of atoms: O10, O8b, and O10a; w3, w1, and w4. The prism is capped on its rectangular faces by O9, w2, and O7b.

Table X. Metal–Ligand Distances (Å) and Angles (deg)[a] for $Mg[Ba(EGTA)]\cdot{}^{8}/_{3}H_2O\cdot{}^{1}/_{3}(CH_3)_2CO$ (3)

a. Complex Ions

complex a		complex b		complex c	
Ba1–N1	2.863 (4)	Ba2–N3	2.924 (4)	Ba3–N5	2.876 (4)
Ba1–N2	2.888 (4)	Ba2–N4	2.935 (4)	Ba3–N6	2.876 (4)
Ba1–O1	2.783 (3)	Ba2–O4	2.815 (3)	Ba3–O14	2.814 (3)
Ba1–O3	2.840 (3)	Ba2–O11	2.827 (3)	Ba3–O21	2.844 (3)
Ba1–O5	2.807 (3)	Ba2–O13	2.811 (3)	Ba3–O23	2.809 (3)
Ba1–O6	2.963 (3)	Ba2–O15	2.832 (3)	Ba3–O25	2.867 (3)
Ba1–O7	2.756 (3)	Ba2–O16	2.803 (3)	Ba3–O26	2.790 (3)
Ba1–O9	2.815 (3)	Ba2–O17	2.759 (3)	Ba3–O27	2.776 (3)
Ba1–O12	2.839 (3)	Ba2–O19	2.822 (3)	Ba3–O29	2.804 (3)
Ba1–$O24_a$	2.839 (3)	Ba2–O22	2.868 (3)	Ba3–$O2_a$	2.799 (3)
N1–Ba1–N2	174.4 (1)	N3–Ba2–N4	176.1 (1)	N5–Ba3–N6	178.0 (1)
N1–Ba1–O1	58.8 (1)	N3–Ba2–O4	86.0 (1)	N5–Ba3–O14	84.9 (1)
N2–Ba1–O1	126.2 (1)	N4–Ba2–O4	94.6 (1)	N6–Ba3–O14	94.5 (1)
N1–Ba1–O3	57.8 (1)	N3–Ba2–O11	57.5 (1)	N5–Ba3–O21	58.1 (1)
N2–Ba1–O3	121.1 (1)	N4–Ba2–O11	126.2 (1)	N6–Ba3–O21	123.3 (1)
O1–Ba1–O3	98.1 (1)	O4–Ba2–O11	63.6(1)	O14–Ba3–O21	64.2 (1)
N1–Ba1–O5	59.0 (1)	N3–Ba2–O13	57.0 (1)	N5–Ba3–O23	58.6 (1)
N2–Ba1–O5	115.9 (1)	N4–Ba2–O13	122.1 (1)	N6–Ba3–O23	121.7 (1)
O1–Ba1–O5	101.0 (1)	O4–Ba2–O13	143.0 (1)	O14–Ba3–O23	142.9 (1)
O3–Ba1–O5	85.9 (1)	O11–Ba2–O13	94.6 (1)	O21–Ba3–O23	98.0 (1)
N1–Ba1–O6	114.9 (1)	N3–Ba2–O15	59.5 (1)	N5–Ba3–O25	61.8 (1)
N2–Ba1–O6	59.9 (1)	N4–Ba2–O15	116.8 (1)	N6–Ba3–O25	116.2 (1)
O1–Ba1–O6	140.5 (1)	O4–Ba2–O15	77.1 (1)	O14–Ba3–O25	74.7 (1)
O3–Ba1–O6	110.4 (1)	O11–Ba2–O15	105.7 (1)	O21–Ba3–O25	107.8 (1)
O5–Ba1–O6	56.2 (1)	O13–Ba2–O15	81.2 (1)	O23–Ba3–O25	81.4 (1)
N1–Ba1–O7	126.0 (1)	N3–Ba2–O16	117.7 (1)	N5–Ba3–O26	119.6 (1)
N2–Ba1–O7	59.0 (1)	N4–Ba2–O16	58.8 (1)	N6–Ba3–O26	58.3 (1)
O1–Ba1–O7	67.2 (1)	O4–Ba2–O16	77.4 (1)	O14–Ba3–O26	75.9 (1)
O3–Ba1–O7	136.6 (1)	O11–Ba2–O16	140.6 (1)	O21–Ba3–O26	140.0 (1)
O5–Ba1–O7	135.7 (1)	O13–Ba2–O16	115.4 (1)	O23–Ba3–O26	114.3 (1)
O6–Ba1–O7	105.0 (1)	O15–Ba2–O16	58.2 (1)	O25–Ba3–O26	58.0 (1)
N1–Ba1–O9	120.6 (1)	N3–Ba2–O17	124.6 (1)	N5–Ba3–O27	122.9 (1)
N2–Ba1–O9	58.1 (1)	N4–Ba2–O17	59.0 (1)	N6–Ba3–O27	58.4 (1)
O1–Ba1–O9	138.1 (1)	O4–Ba2–O17	65.9 (1)	O14–Ba3–O27	64.7 (1)
O3–Ba1–O9	63.0 (1)	O11–Ba2–O17	67.2 (1)	O21–Ba3–O27	65.1 (1)
O5–Ba1–O9	113.6 (1)	O13–Ba2–O17	135.5 (1)	O23–Ba3–O27	139.7 (1)
O6–Ba1–O9	80.7 (1)	O15–Ba2–O17	141.6 (1)	O25–Ba3–O27	137.6 (1)
O7–Ba1–O9	99.9 (1)	O16–Ba2–O17	102.1 (1)	O26–Ba3–O27	99.2 (1)
N1–Ba1–O12	95.1 (1)	N3–Ba2–O19	121.3 (1)	N5–Ba3–O29	122.3 (1)
N2–Ba1–O12	89.0 (1)	N4–Ba2–O19	57.6 (1)	N6–Ba3–O29	58.0 (1)
O1–Ba1–O12	74.5 (1)	O4–Ba2–O19	151.7 (1)	O14–Ba3–O29	151.7 (1)
O3–Ba1–O12	65.5 (1)	O11–Ba2–O19	135.1 (1)	O21–Ba3–O29	134.3 (1)
O5–Ba1–O12	149.6 (1)	O13–Ba2–O19	64.5 (1)	O23–Ba3–O29	63.7 (1)
O6–Ba1–O12	142.1 (1)	O15–Ba2–O19	109.1 (1)	O25–Ba3–O29	109.8 (1)
O7–Ba1–O12	71.2 (1)	O16–Ba2–O19	82.9 (1)	O26–Ba3–O29	83.1 (1)
O9–Ba1–O12	63.6 (1)	O17–Ba2–O19	99.4 (1)	O27–Ba3–O29	101.1 (1)
N1–Ba1–$O24_a$	90.9 (1)	N3–Ba2–O22	94.4 (1)	N5–Ba3–$O2_a$	95.1 (1)
N2–Ba1–$O24_a$	89.6 (1)	N4–Ba2–O22	88.3 (1)	N6–Ba3–$O2_a$	86.9 (1)
O1–Ba1–$O24_a$	64.4 (1)	O4–Ba2–O22	127.6 (1)	O14–Ba3–$O2_a$	126.8 (1)
O3–Ba1–$O24_a$	148.5 (1)	O11–Ba2–O22	72.9 (1)	O21–Ba3–$O2_a$	71.0 (1)
O5–Ba1–$O24_a$	73.0 (1)	O13–Ba2–O22	64.3 (1)	O23–Ba3–$O2_a$	68.4 (1)
O6–Ba1–$O24_a$	77.3 (1)	O15–Ba2–O22	145.0 (1)	O25–Ba3–$O2_a$	148.9 (1)
O7–Ba1–$O24_a$	63.3 (1)	O16–Ba2–O22	142.1 (1)	O26–Ba3–$O2_a$	141.6 (1)
O9–Ba1–$O24_a$	147.2 (1)	O17–Ba2–O22	71.5 (1)	O27–Ba3–$O2_a$	71.5 (1)
O12–Ba1–$O24_a$	127.2 (1)	O19–Ba2–O22	62.4 (1)	O29–Ba3–$O2_a$	63.4 (1)

b. Counterions

counterion 1		counterion 2		counterion 3	
Mg1–O3	2.058 (3)	Mg2–O1	2.171 (3)	Mg3–O13	2.057 (3)
Mg1–O9	2.101 (3)	Mg2–O7	2.111 (3)	Mg3–O19	2.083 (3)
Mg1–O11	2.154 (3)	Mg2–w3	2.080 (3)	Mg3–O21	2.119 (3)
Mg1–O17	2.118 (3)	Mg2–w4	2.083 (3)	Mg3–O27	2.085 (3)
Mg1–w1	2.075 (3)	Mg2–$O23_a$	2.069 (3)	Mg3–w5	2.124 (3)
Mg1–w2	2.040 (3)	Mg2–$O29_a$	2.071 (3)	Mg3–$w6_a$	2.085 (3)
O3–Mg1–O9	90.6 (1)	O1–Mg2–O7	91.4 (1)	O13–Mg2–O19	93.0 (1)
O3–Mg1–O11	83.6 (1)	O1–Mg2–w3	88.9 (1)	O13–Mg3–O21	85.5 (1)
O9–Mg1–O11	92.2 (1)	O7–Mg2–w3	84.7 (1)	O19–Mg3–O21	93.8 (1)
O3–Mg1–O17	94.0 (1)	O1–Mg2–w4	173.2 (1)	O13–Mg3–O27	93.4 (1)
O9–Mg1–O17	173.6 (1)	O7–Mg2–w4	89.2 (1)	O19–Mg3–O27	171.7 (1)
O11–Mg1–O17	92.7 (1)	w3–Mg2–w4	97.9 (1)	O21–Mg3–O27	91.9 (1)
O3–Mg1–w1	170.5 (1)	O1–Mg2–$O23_a$	83.2 (1)	O13–Mg3–w5	88.1 (1)
O9–Mg1–w1	91.0 (1)	O7–Mg2–$O23_a$	94.8 (1)	O19–Mg3–w5	86.2 (1)
O11–Mg1–w1	86.9 (1)	w3–Mg2–$O23_a$	172.0 (1)	O21–Mg3–w5	173.6 (1)
O17–Mg1–w1	85.2 (1)	w4–Mg2–$O23_a$	90.0 (1)	O27–Mg3–w5	88.7 (1)

Table X (Continued)

counterion 1		counterion 2		counterion 3	
O3–Mg1–w2	93.8 (1)	O1–Mg2–O29$_a$	89.2 (1)	O13–Mg3–w6$_a$	173.0 (1)
O9–Mg1–w2	86.7 (1)	O7–Mg2–O29$_a$	173.9 (1)	O19–Mg3–w6$_a$	90.1 (1)
O11–Mg1–w2	177.2 (1)	w3–Mg2–O29$_a$	89.2 (1)	O21–Mg3–w6$_a$	88.1 (1)
O17–Mg1–w2	88.6 (1)	w4–Mg2–O29$_a$	90.9 (1)	O27–Mg3–w6$_a$	84.1 (1)
w1–Mg1–w2	95.7 (1)	O23$_a$–Mg2–O29$_a$	91.3 (1)	w5–Mg3–w6$_a$	98.3 (1)
		c. Interionic Angles			
Ba1–O1–Mg2	99.5 (1)	Ba2–O11–Mg1	98.5 (1)	Mg3–O21–C30	124.0 (3)
Mg2–O1–C2	128.7 (3)	Mg1–O11–C16	126.4 (3)	Ba3–O23–Mg2$_a$	102.4 (1)
C2–O2–Ba3$_a$	134.0 (3)	Ba2–O13–Mg3	101.7 (1)	C32–O23–Mg2$_a$	125.2 (3)
Ba1–O3–Mg1	103.3 (1)	Mg3–O13–C18	126.7 (3)	C32–O24–Ba1$_a$	135.9 (3)
Mg1–O3–C4	127.0 (3)	Ba2–O17–Mg1	101.5 (1)	Ba3–O27–Mg3	102.9 (1)
Ba1–O7–Mg2	101.9 (1)	Mg1–O17–C26	130.3 (3)	Mg3–O27–C40	128.5 (3)
Mg2–O7–C12	126.3 (3)	Ba2–O19–Mg3	100.7 (1)	Ba3–O29–Mg2$_a$	102.5 (1)
Ba1–O9–Mg1	103.0 (1)	Mg3–O19–C28	127.7 (3)	C42–O29–Mg2$_a$	126.3 (3)
Mg1–O9–C14	125.0 (3)	Ba3–O21–Mg3	99.9 (1)		

[a] Estimated standard deviations in the least significant digits are given in parentheses.

Table XI. Chelate Ring[a] Bonding Parameters[b] for Mg[Ba(EGTA)]·$^8/_3H_2O$·$^1/_3(CH_3)_2CO$ (**3**)

Glycinate Rings

	C–C′	C′–N	C–O	C–O′	C–C′–N	O–C–O′	C′–C–O	C′–C–O′	Ba–N–C′	Ba–O–C
G1	1.534 (6)	1.460 (5)	1.267 (5)	1.246 (5)	114.6 (3)	126.2 (4)	118.6 (3)	115.1 (3)	110.0 (3)	120.1 (2)
G2	1.526 (6)	1.459 (6)	1.269 (6)	1.241 (5)	115.5 (4)	126.8 (4)	117.0 (4)	116.1 (4)	104.1 (2)	137.6 (3)
G3	1.522 (7)	1.458 (6)	1.275 (5)	1.254 (6)	115.7 (4)	125.8 (4)	119.1 (4)	115.1 (4)	110.0 (3)	119.3 (3)
G4	1.511 (6)	1.467 (5)	1.270 (5)	1.246 (5)	115.0 (4)	124.3 (4)	118.7 (4)	117.0 (4)	103.3 (2)	114.4 (3)
G5	1.525 (6)	1.461 (5)	1.270 (5)	1.250 (5)	114.7 (3)	126.4 (4)	118.5 (4)	115.0 (4)	108.8 (2)	135.4 (3)
G6	1.531 (6)	1.470 (5)	1.273 (5)	1.243 (5)	114.2 (3)	127.1 (4)	117.4 (3)	115.5 (4)	106.6 (2)	138.8 (3)
G7	1.525 (7)	1.474 (6)	1.259 (6)	1.256 (6)	114.0 (4)	124.3 (4)	119.6 (4)	116.1 (4)	109.0 (2)	123.9 (3)
G8	1.538 (6)	1.475 (6)	1.255 (5)	1.241 (5)	113.7 (4)	126.5 (4)	117.1 (4)	116.4 (4)	105.0 (2)	121.2 (3)
G9	1.533 (6)	1.466 (5)	1.275 (5)	1.245 (5)	114.8 (3)	125.4 (4)	119.0 (3)	115.5 (3)	112.2 (2)	136.8 (3)
G10	1.545 (6)	1.460 (5)	1.270 (5)	1.243 (5)	116.0 (4)	126.7 (4)	117.1 (3)	116.1 (4)	105.5 (2)	116.3 (2)
G11	1.512 (6)	1.474 (5)	1.270 (5)	1.249 (5)	114.2 (3)	125.6 (4)	119.0 (4)	115.4 (4)	110.8 (2)	121.6 (3)
G12	1.519 (6)	1.465 (5)	1.279 (5)	1.259 (5)	113.7 (4)	125.1 (4)	120.8 (10)	116.8 (4)	102.3 (2)	114.6 (2)

Amino–Ether Rings

	C–C′	C–N	C′–O	C–C′–O	C′–C–N	C″–N–C†	C–N–C″	C–N–C†	Ba–N–C	Ba–O–C′
A1	1.502 (7)	1.472 (6)	1.423 (6)	109.3 (4)	112.4 (4)	108.9 (4)	111.3 (3)	111.2 (3)	111.0 (3)	123.5 (3)
A2	1.515 (6)	1.474 (6)	1.442 (6)	108.8 (4)	113.6 (3)	109.5 (4)	111.3 (3)	110.2 (3)	112.2 (3)	117.1 (3)
A3	1.506 (7)	1.477 (6)	1.406 (6)	108.9 (4)	112.7 (4)	109.4 (3)	112.3 (3)	109.0 (3)	110.5 (3)	121.5 (3)
A4	1.509 (7)	1.471 (6)	1.421 (6)	109.6 (4)	113.4 (4)	110.5 (4)	111.8 (3)	108.6 (3)	111.8 (3)	124.9 (3)
A5	1.514 (7)	1.471 (6)	1.436 (6)	109.2 (3)	113.2 (4)	108.3 (3)	110.5 (3)	110.1 (3)	110.2 (2)	115.2 (3)
A6	1.519 (6)	1.466 (6)	1.441 (6)	107.8 (4)	112.5 (4)	110.7 (3)	110.5 (3)	110.0 (3)	112.2 (3)	125.9 (3)

Diether Rings

	C–C′	C′–O′	C–O	C′–C–O	C–C′–O′	C′–O′–C†	C″–O–C	Ba–O–C	Ba–O′–C′
E1	1.495 (7)	1.447 (5)	1.439 (6)	109.0 (4)	109.6 (4)	111.0 (3)	112.4 (4)	123.6 (3)	104.4 (3)
E2	1.480 (7)	1.448 (6)	1.427 (6)	109.5 (4)	109.0 (4)	113.7 (4)	111.7 (3)	114.4 (3)	121.3 (3)
E3	1.501 (8)	1.410 (7)	1.425 (6)	108.9 (4)	110.6 (4)	111.8 (4)	111.0 (3)	110.3 (3)	122.2 (3)

[a] Chelate ring designations have been assigned systematically, as described in Table V. [b] Bond lengths are given in angstroms and bond angles in degrees. Estimated standard deviations in the least significant digits are given in parentheses.

Except for the long bond to O7a (see above), the bridging bond lengths to strontium range from 2.588 (4) to 2.703 (3) Å, with Sr–O(carboxylate)(av) = 2.65 (6) Å. Despite the fact that O10 is involved in both bidentate and unidentate(O′) bridges, the unidentate(O′) bridge exhibits the shortest Sr–O(carboxylate) distance (2.588 (4) Å). The average Sr–O(carboxylate) distance seen in Mg[Sr(EGTA)(OH_2)]·$7H_2O$ (**2**, see below) is 2.67 (6) Å, with a range of 2.588 (4)–2.722 (5) Å. The lack of any dependence of Sr–O(carboxylate) distances on the location of the Sr^{2+} ion (counterion or complex anion) is surprising.

Compound **1**, like **5**, is held together in the solid state by carboxylate bridges between metal ions and by hydrogen bonding. Two occluded water molecules participate in hydrogen bonding with carboxylate groups and coordinated water molecules to link the polymeric cation–anion chains, which are propagated parallel to the *a* axis. As in **5**, all carboxylate oxygen atoms are involved in at least one interaction with a metal ion or a water molecule.

The different bridging interactions in **1** and **5** do not influence the mean Ca^{2+}–ligand bonding parameters—for **1**, Ca–N(av) = 2.592 (9) Å, Ca–O(carboxylate)(av) = 2.377 (8) Å, and Ca–O(ether)(av) = 2.51 (2) Å; for **5**, Ca–N(av) = 2.60 (2) Å, Ca–O(carboxylate)(av) = 2.38 (2) Å, and Ca–O(ether)(av) = 2.50 (3) Å. While there are slight differences in the ways in which the $EGTA^{4-}$ ligands wrap around the Ca^{2+} ions in the two structures, as judged by chelate ring and inter-ring torsion angles (see supplementary material), it appears that the differences in bridging interactions do not perturb the chelation of Ca^{2+} by $EGTA^{4-}$ in any significant fashion. In fact, the conformations of calcium, cadmium(II),[12] and high-spin manganese(II)[16] complexes differ only slightly, and it now appears that there is relatively little variability in how the $EGTA^{4-}$ ligand wraps around a metal ion to form an eight-coordinate chelate. Changes in the nature of the neutral ligand atoms have immediate consequences, however. In the eight-coordinate $[Ca(FBAPTA)]^{2-}$ complex anion (H_4FBAPTA = 5,5′-difluoro-1,2-bis(*o*-aminophenoxy)ethane-*N*,*N*,*N*′,*N*′-tetraacetic acid), Ca–N(av) = 2.654 (8) Å, Ca–O-

(16) Schauer, C. K.; Anderson, O. P. *Acta Crystallogr., Sect. C: Cryst. Struct. Commun.*, in press.

Table XII. Atomic Coordinates (Fractional, $\times 10^4$) and Equivalent Isotropic Thermal Parameters ($Å^2 \times 10^3$) for $[Mg_2(EGTA)(OH_2)_6]\cdot 5H_2O$ (**4**)[a]

atom	x	y	z	U_{iso}[b]
Mg1	8876 (1)	6742 (1)	3088 (1)	24 (1)
Mg2	6146 (1)	6556 (1)	10902 (1)	22 (1)
C1	7808 (3)	7440 (4)	4677 (3)	35 (1)
C2	7297 (3)	7799 (3)	3888 (3)	27 (1)
C3	9527 (3)	7406 (4)	4832 (3)	34 (1)
C4	9862 (3)	8245 (4)	4196 (3)	32 (1)
C5	8644 (4)	5704 (4)	4875 (3)	36 (1)
C6	8762 (4)	5597 (4)	5820 (4)	44 (2)
C7	7173 (4)	5687 (5)	6328 (3)	42 (2)
C8	6579 (5)	6401 (6)	6859 (4)	45 (2)
C8′	7109 (18)	4779 (15)	7007 (11)	43 (7)
C9	6461 (5)	5597 (6)	8148 (4)	65 (2)
C10	6631 (4)	5726 (4)	9102 (3)	40 (2)
C11	7070 (3)	7598 (4)	9383 (3)	32 (1)
C12	7624 (3)	7855 (3)	10171 (3)	24 (1)
C13	5426 (3)	7151 (4)	9204 (3)	28 (1)
C14	5007 (3)	7939 (4)	9831 (3)	27 (1)
N1	8693 (2)	6816 (3)	4534 (2)	24 (1)
N2	6358 (2)	6762 (3)	9491 (2)	22 (1)
O1	7566 (2)	7462 (3)	3191 (2)	34 (1)
O2	6615 (3)	8412 (3)	4012 (2)	42 (1)
O3	9653 (2)	8091 (3)	3437 (2)	33 (1)
O4	10351 (3)	9013 (3)	4465 (3)	49 (1)
O5	8087 (2)	6180 (3)	6306 (2)	39 (1)
O6	6869 (3)	6389 (4)	7724 (3)	39 (1)
O6′	7287 (8)	5180 (10)	7796 (7)	28 (4)
O7	7399 (2)	7390 (3)	10848 (2)	30 (1)
O8	8277 (2)	8548 (3)	10100 (2)	34 (1)
O9	5286 (2)	7869 (2)	10585 (2)	27 (1)
O10	4414 (2)	8599 (3)	9570 (2)	41 (1)
w1	10140 (2)	5937 (3)	3100 (2)	38 (1)
w2	8212 (2)	5274 (3)	2978 (3)	42 (1)
w3	8928 (2)	7071 (3)	1847 (2)	42 (1)
w4	4924 (2)	5612 (2)	10763 (2)	33 (1)
w5	6846 (2)	5100 (3)	10983 (3)	38 (1)
w6	6052 (2)	6804 (3)	12156 (2)	36 (1)
w7	8654 (2)	4684 (3)	418 (3)	42 (1)
w8	3517 (3)	5384 (3)	8600 (3)	46 (1)
w9	9067 (4)	3840 (4)	2010 (3)	72 (2)
w10	6220 (5)	3559 (4)	12043 (4)	92 (2)
w11	10849 (3)	3796 (4)	2873 (3)	57 (1)

[a] Estimated standard deviations in the least significant digits are given in parentheses. [b] The equivalent isotropic U is equal to one-third of the trace of the U_{ij} tensor.

(carboxylate)(av) = 2.34 (2) Å, and Ca–O(ether)(av) = 2.67 (6) Å.[17]

Structure of $Mg[Sr(EGTA)(OH_2)]\cdot 7H_2O$ (2). The Sr^{2+} ion in the $[Sr(EGTA)]^{2-}$ chelate in **2** is nine-coordinate (see Figure 3). In addition to the eight coordinating atoms from the $EGTA^{4-}$ ligand, a water molecule (w1) is strongly bound to the strontium ion (Sr–w1 = 2.554 (5) Å). The ligand atoms about Sr^{2+} occupy the vertices of a slightly distorted tricapped trigonal prism. The trigonal faces of the prism are comprised of O7, O6, and O9 and of O1, O5, and O3. Capping of the trigonal faces is accomplished by the nitrogen atoms of the $EGTA^{4-}$ ligand. The water molecule, w1, caps the rectangular face made up of O9, O7, O3, and O1. As a consequence of the geometric constraints arising from the carboxylate bridges between $[Sr(EGTA)]^{2-}$ and Mg2 (see below and Figure 4), one of the water molecules already bound to a magnesium counterion is brought into relatively close proximity to the strontium ion (Sr–w2 = 2.970 (5) Å). If w2 is considered to be part of the coordination sphere of the Sr^{2+} ion, it occupies a position that also caps a rectangular face (O6, O5, O7, and O3).

Magnesium ion was chosen as the counterion because of a previously observed tendency to remain as a discrete hexaaqua ion rather than form bridges to carboxylate oxygen atoms of metal chelates.[18] This did not prove to be the case in **2** (nor was it the case in **3**; see below). In **2**, two crystallographically unique Mg^{2+} counterions appear in the asymmetric unit of the unit cell. Mg1 occupies a special position of $\bar{1}$ symmetry, while Mg2 resides on a site of 2 symmetry. The coordination sphere for each Mg^{2+} ion

Table XIII. Metal–Ligand Distances (Å) and Angles (deg)[a] for $[Mg_2(EGTA)(OH_2)_6]\cdot 5H_2O$ (**4**)

complex a		complex b	
Mg1–N1	2.318 (4)	Mg2–N2	2.281 (4)
Mg1–O1	2.057 (3)	Mg2–O7	2.047 (3)
Mg1–O3	2.076 (3)	Mg2–O9	2.092 (3)
Mg1–w1	2.043 (3)	Mg2–w4	2.095 (3)
Mg1–w2	2.054 (4)	Mg2–w5	2.061 (3)
Mg1–w3	2.020 (4)	Mg2–w6	2.025 (4)
N1–Mg1–O1	78.7 (1)	N2–Mg2–O7	77.8 (1)
N1–Mg1–O3	76.2 (1)	N2–Mg2–O9	75.6 (1)
O1–Mg1–O3	95.9 (1)	O7–Mg2–O9	95.6 (1)
N1–Mg1–w1	96.2 (1)	N2–Mg2–w4	93.8 (1)
O1–Mg1–w1	173.9 (2)	O7–Mg2–w4	170.7 (2)
O3–Mg1–w1	86.0 (1)	O9–Mg2–w4	86.1 (1)
N1–Mg1–w2	94.0 (2)	N2–Mg2–w5	95.5 (1)
O1–Mg1–w2	89.0 (1)	O7–Mg2–w5	91.8 (1)
O3–Mg1–w2	167.8 (2)	O9–Mg2–w5	166.9 (2)
w1–Mg1–w2	88.0 (1)	w4–Mg2–w5	84.9 (1)
N1–Mg1–w3	165.5 (2)	N2–Mg2–w6	164.4 (1)
O1–Mg1–w3	91.3 (1)	O7–Mg2–w6	91.2 (1)
O3–Mg1–w3	94.6 (2)	O9–Mg2–w6	94.7 (1)
w1–Mg1–w3	94.3 (2)	w4–Mg2–w6	97.8 (1)
w2–Mg1–w3	96.4 (2)	w5–Mg2–w6	95.9 (2)

[a] Estimated standard deviations in the least significant digits are given in parentheses.

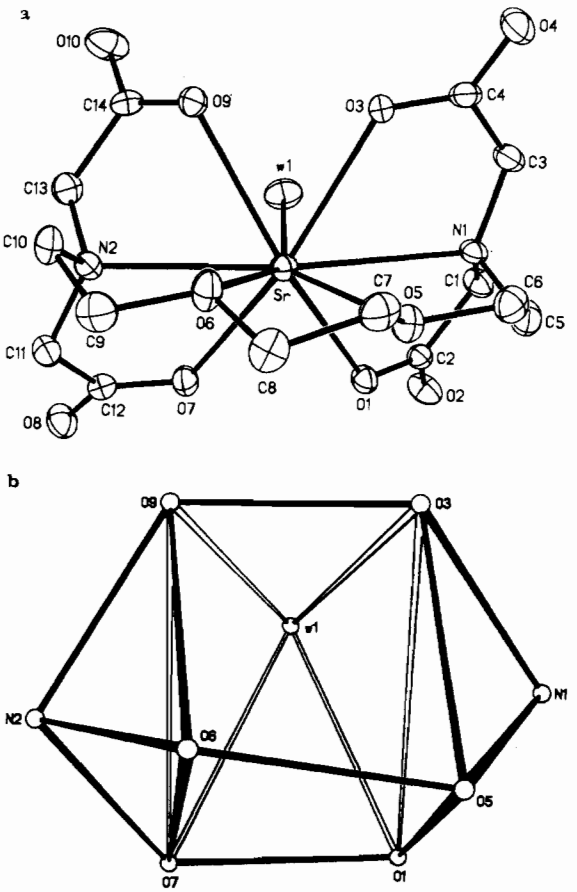

Figure 3. (a) Thermal ellipsoid plot (50%) of the $[Sr(EGTA)(OH_2)]^{2-}$ complex ion in **2**. (b) View of the coordination polyhedron about Sr^{2+} in **2**.

(17) Gerig, J. T.; Singh, P.; Levy, L. A.; London, R. E. *J. Inorg. Biochem.* **1987**, *31*, 113.

(18) Bozhidaev, A. I.; Polynova, T. N.; Porai-Koshits, M. A. *Acta Crystallogr., Sect. A: Cryst. Phys., Diffr., Theor. Gen. Crystallogr.* **1972**, *A28*, S76.

Table XIV. Chelate Ring[a] Bonding Parameters[b] for $[Mg_2(EGTA)(OH_2)_6]\cdot 5H_2O$ (4)

Glycinate Rings

	C–C′	C′–N	C–O	C–O′	C–C′–N	O–C–O′	C′–C–O	C′–C–O′	Mg–N–C′	Mg–O–C
G1	1.516 (6)	1.486 (6)	1.246 (6)	1.241 (5)	115.1 (4)	125.8 (4)	119.7 (4)	114.5 (4)	105.5 (2)	119.4 (3)
G2	1.527 (7)	1.464 (6)	1.258 (6)	1.252 (6)	111.9 (4)	124.9 (5)	117.6 (4)	117.5 (4)	104.6 (3)	120.1 (3)
G3	1.513 (6)	1.453 (6)	1.262 (5)	1.265 (5)	114.1 (4)	124.8 (4)	118.9 (4)	116.4 (4)	106.6 (3)	118.9 (3)
G4	1.516 (6)	1.472 (5)	1.267 (5)	1.241 (5)	110.8 (3)	124.8 (4)	117.4 (4)	117.8 (4)	103.0 (2)	117.5 (3)

Amino–Ether Rings

	C–C′	C–N	C′–O	C–C′–O	C′–C–N	C″–N–C†	C–N–C″	C–N–C†	Mg–N–C
A1	1.519 (8)	1.483 (6)	1.425 (7)	114.9 (4)	116.1 (4)	111.3 (3)	112.9 (3)	112.5 (3)	109.4 (3)
A2	1.546 (8)	1.477 (6)	1.323 (8)	111.0 (5)	117.4 (5)	110.3 (3)	113.0 (3)	112.8 (3)	110.5 (3)

Diether Rings

	C–C′	C′–O′	C–O	C′–C–O	C–C′–O′	C′–O′–C†	C″–O–C
E1	1.483 (9)	1.437 (8)	1.426 (6)	105.6 (5)	112.3 (6)	111.9 (5)	113.5 (4)

[a] Chelate ring designations have been assigned systematically, as described in Table V. [b] Bond lengths are given in angstroms and bond angles in degrees. Estimated standard deviations in the least significant digits are given in parentheses.

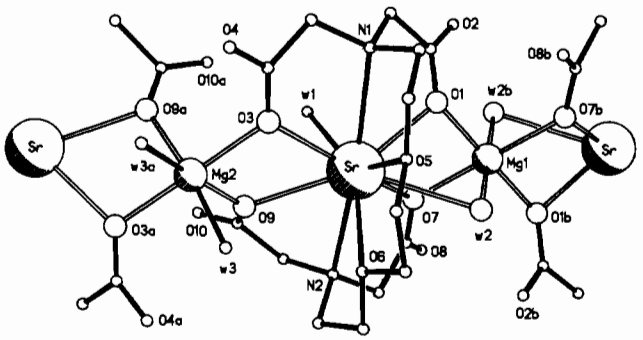

Figure 4. Ball and stick plot depicting the interionic interactions in the solid state for **2**. Conventions are the same as in Figure 2.

is octahedral and consists of two water molecules and the oxygen atoms of four carboxylate groups from $[Sr(EGTA)(OH_2)]^{2-}$ complex anions. The water molecules coordinated to Mg1 occupy trans positions, as required by the crystallographic $\bar{1}$ symmetry. For Mg2, the crystallographically required 2-fold site symmetry is satisfied by a cis arrangement of the two water molecules.

All oxygen atoms that bridge to Mg^{2+} ions in **2** do so via unidentate(O) carboxylate bridges (see Figure 4). The strontium chelate engages in two such bridging interactions to each magnesium ion. As a result, every carboxylate group bound to the Sr^{2+} ion is also bound to a Mg^{2+} ion. The interionic linkages between the strontium chelate and the Mg^{2+} counterions result in the formation of polymeric cation–complex anion chains propagated by the *n* glide parallel to the *xy* plane. These chains are linked by an extensive hydrogen-bonding network; all four of the carboxylate oxygen atoms that are not involved in metal ion coordination (O2, O4, O8, and O10) form hydrogen bonds with occluded water molecules or with water molecules coordinated to Mg^{2+} ions in adjacent polymeric chains. A hydrogen bond between w2 and an occluded water molecule (w5) creates an additional interchain linkage.

Of the three types of oxygen donors to Sr^{2+} in **2**, the water molecule is bound at the shortest distance (Sr–w1 = 2.554 (5) Å). This distance agrees well with previously observed Sr–OH_2 distances.[19] Both Ca^{2+} and Cd^{2+} ion exhibited a preference to bind anionic carboxylate oxygen atoms rather than neutral ether oxygen atoms in the $EGTA^{4-}$ chelates (bond length differences: Cd–O(ether)(av) − Cd–O(carboxylate)(av) = 0.23 Å; Ca–O(ether)(av) − Ca–O(carboxylate)(av) = 0.14 Å).[12] Such a preference is not exhibited by strontium ion. The range of bonding distances observed for the four carboxylate oxygen atoms (2.588 (4)–2.722 (5) Å) actually encompasses the two Sr–O(ether) bond distances (Sr–O5 = 2.605 (4) Å, Sr–O6 = 2.654 (5) Å). The Sr–O(ether) bond distances in **2** are similar to the Sr–O distances observed in two strontium crown ether complexes (for the nine-coordinate Sr^{2+} ion in $[Sr(benzo\text{-}18\text{-}crown\text{-}6)(OH_2)_3](ClO_4)_2$,[19] Sr–O(ether) = 2.662 (5)–2.723 (4) Å and Sr–O(ether)(av) = 2.68 (4) Å; for two independent eight-coordinate Sr^{2+} ions in Sr(4′-acetobenzo-18-crown-6)$(ClO_4)_2$,[20] Sr–O(ether) = 2.61 (2)–2.78 (2) Å and Sr–O(ether)(av) = 2.68 (6) Å). The range of Sr–O(carboxylate) distances seen for the nine-coordinate Sr^{2+} ion in strontium malonate[21] (Sr–O(carboxylate) = 2.512 (3)–2.796 (2) Å, Sr–O(carboxylate)(av) = 2.6 (1) Å) is even larger than that in **2**. Of the four ligand atom types, the amine nitrogen atoms are bound at the longest distances to the strontium ion (Sr–N1 = 2.891 (5) Å, Sr–N2 = 2.802 (5) Å). These distances are very similar to those in the eight-coordinate strontium complex $\{[N(CH_2CH_2OH)_3]_2Sr\}(NO_3)_2$ (Sr–N = 2.830 (4) Å).[22]

A recent review of the literature indicated that Mg^{2+} exhibits a smaller range of metal–water bond distances than does Ca^{2+}.[23] Given this fact, a magnesium counterion might be expected to perturb the coordination sphere about the chelated metal ion more than either Sr^{2+} or Ca^{2+} counterions. The range of Mg–O(carboxylate) distances observed for bridging to magnesium ions in **2** (1.978 (4)–2.094 (4) Å), Mg–O(carboxylate)(av) = 2.05 (5) Å) is relatively small in comparison to the corresponding ranges observed for bridging to Ca^{2+} and Sr^{2+} counterions in other $EGTA^{4-}$ chelates. One must assume that the metal–ligand distances and chelate ring conformational parameters might be influenced by these strong bridging interactions.

Structure of $Mg[Ba(EGTA)]\cdot{}^8/_3H_2O\cdot{}^1/_3(CH_3)_2CO$ (3). The asymmetric unit of the unit cell contains three unique $[Ba(EGTA)]^{2-}$ complex anions (anion a, containing Ba1, is shown in Figure 5). All of the Ba^{2+} ions in **3** are clearly 10-coordinate, in contrast to the Sr^{2+} ion in **2**. In each of the crystallographically unique Ba^{2+}–$EGTA^{4-}$ chelates, all eight ligand atoms of $EGTA^{4-}$ are bound to Ba^{2+}. The two additional ligand atoms in each case are provided through bridging interactions with adjacent Ba^{2+} chelates (see Figure 6 and discussion below). The coordination geometry about Ba^{2+} is based on a trigonal prism; O12 caps the rectangular face that was capped by w1 in the strontium chelate, and O22 caps the O6–O5–O1–O7 face. In **2**, a water molecule was found in the vicinity of this tenth coordination site.

All three of the crystallographically unique Mg^{2+} counterions are six-coordinate and octahedral. The coordination array about each Mg^{2+} ion resembles that about Mg2 in **2**. A noncrystallographic approximate 2-fold axis bisects the w1–Mg1–w2 and

(19) Hughes, D. L.; Mortimer, C. L.; Truter, M. R. *Inorg. Chim. Acta* **1978**, *29*, 43.
(20) Fenton, D. E.; Parkin, D.; Newton, R. F.; Nowell, I. W.; Walker, P. E. *J. Chem. Soc., Dalton Trans.* **1982**, 327.
(21) Briggman, B.; Oskarsson, Å. *Acta Crystallogr., Sect. B: Struct. Crystallogr. Cryst. Chem.* **1977**, *B33*, 1900.
(22) Voegele, J. C.; Fischer, J.; Weiss, R. *Acta Crystallogr., Sect. B: Struct. Crystallogr. Cryst. Chem.* **1974**, *B30*, 66.
(23) Einspahr, H.; Bugg, C. E. In ref 2b, Chapter 2, p 51.

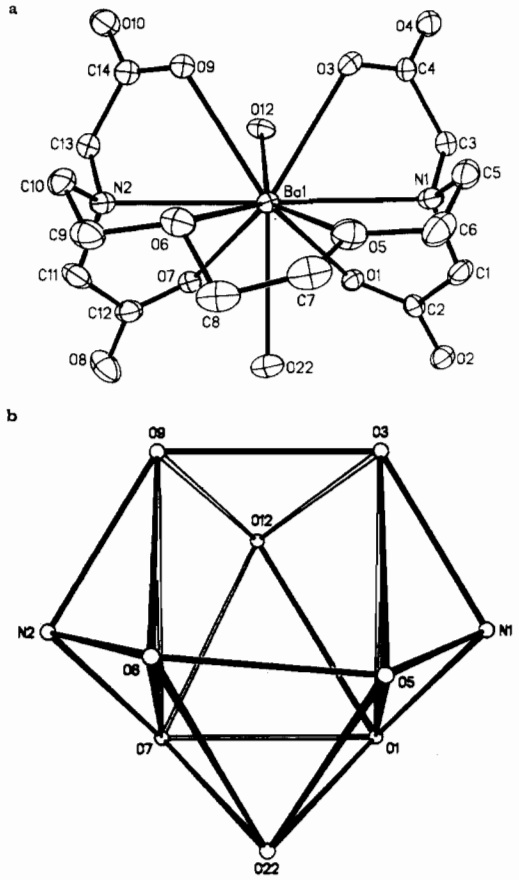

Figure 5. (a) Thermal ellipsoid plot (50%) of the Ba^{2+}–$EGTA^{4-}$ chelate in **3** that involves Ba1. The numbering scheme for the complex anions involving Ba2 and Ba3 may be derived as follows: for Cx, $x = 14(n-1) + a$; for Ox, $x = 10(n-1) + a$; for Nx, $x = 2(n-1) + a$; n = complex anion number, a = atom number in the complex involving Ba1. (b) View of the coordination polyhedron about Ba^{2+} in **3**.

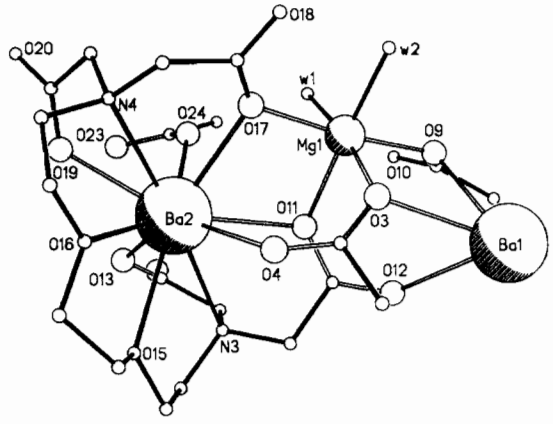

Figure 6. Ball and stick plot depicting the interionic interactions in the solid state for **3**. Conventions are the same as in Figure 2.

O11–Mg1–O3 angles. Two of the four carboxylate groups of the $EGTA^{4-}$ ligands simultaneously act as unidentate(O′) and unidentate(O) bridging donors to adjacent Ba^{2+} complexes and Mg^{2+} counterions, respectively (see, for example, the carboxylate group containing O3 and O4, which is part of the ligand chelating Ba1 and bridges to Ba2 and Mg1). The remaining two carboxylate groups only bridge in a unidentate(O) fashion to the Mg^{2+} counterions (see, for example, O17 bridging to Mg1). The Mg–O(carboxylate) distances for the three unique Mg^{2+} counterions in **3** (2.057 (3)–2.171 (3) Å, Mg–O(carboxylate)(av) = 2.10 (4) Å) are longer than the Mg–O(carboxylate) bridge distances seen in **2**.

The barium–EGTA chelates and partially aquated Mg^{2+} counterions link together to form polymeric ribbons parallel to the *ab* plane. The ribbons are held together in the *z* direction by hydrogen bonding between the eight occluded water molecules in the asymmetric unit and carboxylate oxygen atoms O14, O10, and O18. The occluded acetone molecule is also located between these polymeric ribbons.

The Ba–O(carboxylate) bond distances do not seem to be influenced by the bridging or nonbridging nature of the carboxylate groups. The range of intrachelate distances seen (Ba–O(carboxylate) = 2.756 (3)–2.844 (3) Å, Ba–O(carboxylate)(av) = 2.80 (3) Å) is very similar to the range of interchelate distances seen (Ba–O(carboxylate) = 2.799 (3)–2.868 (3) Å, Ba–O(carboxylate)(av) = 2.83 (2) Å). Surprisingly, the carboxylate groups that are engaged in both unidentate(O′) and unidentate(O) bridging interactions are not bound more weakly to the Ba^{2+} ion of the barium–EGTA chelates.

As did the Sr^{2+} ion in **2**, the Ba^{2+} ion exhibits no distinct preference for the neutral ether oxygen or anionic carboxylate oxygen donors of the $EGTA^{4-}$ ligand. With the exception of one long Ba–O(ether) distance (Ba1–O6 = 2.963 (3) Å), the range of Ba–O(ether) distances (2.790 (3)–2.867 (3) Å, Ba–O(ether)(av) = 2.82 (3) Å) is similar to the range of Ba–O(carboxylate) distances. A conformational change in the diether ring of complex a is associated with the unusually long Ba1–O6 distance (see below). The Ba–O(ether) distances are similar to those in 10-coordinate $[Ba(benzo\text{-}18\text{-}crown\text{-}6)(OH_2)_2](ClO_4)_2$ (Ba–O(ether) = 2.802 (6)–2.846 (5) Å, Ba–O(ether)(av) = 2.82 (2) Å).[19] In the reported structure of $Ba[Ba(EDTA)]\cdot 2.5H_2O$,[24] the poor precision and extremely large variation in chemically equivalent bond lengths make comparisons of little value; thus, no reliable comparative data exist for the Ba–O(carboxylate) bond lengths in **3**.

The amine nitrogen atoms are bound at a slightly longer distance than are the oxygen atoms (Ba–N = 2.863 (4)–2.935 (4) Å, Ba–N(av) = 2.89 (3) Å). These distances are shorter than those in 10-coordinate $[Ba(2.2.2)(OH_2)(SCN)]^+$ (Ba–N = 2.88 (1)–3.00 (1) Å, Ba–N(av) = 2.95 (5) Å)[25] by an amount (0.06 Å) that is consistent with the change in coordination number.[26]

The δ/λ conformations of corresponding individual chelate rings in the three crystallographically unique $[Ba(EGTA)]^{2-}$ complexes in **3** are identical, with one exception. The diether ring of complex a exhibits a λ configuration, whereas the same rings in complexes b and c exhibit δ configurations. At the same time, one of the ether oxygen atoms in complex a is bound to Ba^{2+} at a relatively long distance (see above). Complex a is not involved in hydrogen-bonding or bridging interactions significantly different from those of complexes b and c, but the presence of the occluded acetone molecule in the vicinity of complex a may cause this difference (a methyl hydrogen atom of the occluded acetone molecule is in van der Waals contact with a hydrogen atom on C7 in complex a).

One of the ether oxygen atoms in the N–O–O–N belt of $EGTA^{4-}$ coordinates to Ba^{2+} by using both lone pairs (a phenomenon also observed in the $[Nd(EGTA)]^-$ complex anion[1] and referred to as "planar" ether oxygen binding). The displacement of Ba^{2+} from the plane containing the ether oxygen atom and the two carbon atoms bound to it makes this clear; this displacement for amino–ether rings A1, A4, and A6 (0.34, 0.21, and 0.10 Å, respectively) is quite different than for rings A2, A3, and A5 (2.29, 1.55, and 2.09 Å, respectively). In addition, the angle the Ba–O(ether) vector makes with the normal to the C–O–C plane should be 90° for an ether oxygen atom that utilizes both lone pairs equally in coordinating to the metal ion. The angles for the ether oxygen atoms with small out-of-plane displacements are 97° (A1), 86° (A4), and 92° (A6), while those for the ether oxygen atoms with large out-of-plane displacements are 141° (A2), 127° (A3), and 137° (A5).

(24) Shao, M. C.; Tang, Z.-R.; Liu, T.-C.; Song, S.-Y.; Tang, Y.-Q. *Sci. Sin. (Engl. Ed.)* **1979**, *22*, 912.
(25) Metz, B.; Moras, D.; Weiss, R. *Acta Crystallogr., Sect. B: Struct. Crystallogr. Cryst. Chem.* **1973**, *B29*, 1382.
(26) Shannon, R. D. *Acta Crystallogr., Sect. A: Cryst. Phys., Diffr., Theor. Gen. Crystallogr.* **1976**, *A32*, 751.

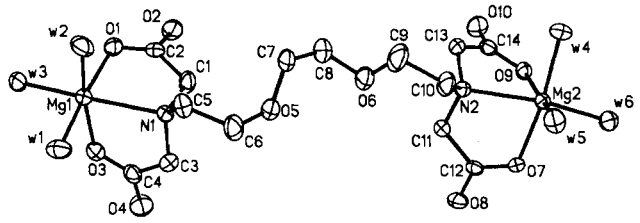

Figure 7. Thermal ellipsoid plot (50%) of the dinuclear $[Mg_2(EGTA)(OH_2)_6]$ complex in **4**.

The structures of two barium cryptate complexes reveal that such "planar" coordination of an ether oxygen atom in an N–O–O–N ring system is not unusual. In 11-coordinate $[Ba(3.2.2)(OH_2)_2]^{2+}$,[27] the two N–O–O–N ring systems each contain such a "planar" ether oxygen atom. In 10-coordinate $[Ba(2.2.2)(OH_2)(NCS)]^{+}$,[28] one of the three N–O–O–N belts exhibits such a "planar" oxygen atom. Since the cryptate complexes are not involved in interionic interactions, as are the barium chelates in **3**, the adoption of a "planar" configuration at oxygen is probably necessary to relieve accumulated strain in the formation of five-membered rings with the large Ba^{2+} ion.

Structure of $[Mg_2(EGTA)(OH_2)_6]\cdot 5H_2O$ (4). Reaction of 2 equiv of a magnesium salt with $EDTA^{4-}$ yields a crystalline compound that contains a $[Mg(OH_2)_6]^{2+}$ cation and a seven-coordinate $[Mg(EDTA)(H_2O)]^{2-}$ complex anion.[29] The analogous reaction with $EGTA^{4-}$ instead yields a neutral, dinuclear product, in which each end of the $EGTA^{4-}$ ligand acts as a tridentate amino–dicarboxylate ligand (see Figure 7). Three water molecules complete the ligand array for the six-coordinate, octahedral Mg^{2+} ions. The two oxygen atoms of the tridentate $EGTA^{4-}$ fragment occupy cis sites in each of the octahedra. Crystals of **4** have been isolated repeatedly from reaction mixtures in which the $Mg^{2+}/EGTA^{4-}$ stoichiometry is 1/1.

The bonding parameters that describe the coordination spheres of the Mg^{2+} ions are not unusual. The water molecules and the carboxylate oxygen atoms are bound at approximately the same distances (Mg–O(carboxylate)(av) = 2.07 (2) Å, Mg–O(water)(av) = 2.05 (3) Å), while the amine nitrogen atoms are bound at a considerably longer distance (Mg–N(av) = 2.30 (3) Å). In seven-coordinate $[Mg(EDTA)(OH_2)]^{2-}$,[29-31] the amine nitrogen atoms are bound at a longer distance still (Mg–N = 2.378 (2) Å), while the carboxylate groups and the water molecule are bound at distances (Mg–O(carboxylate) = 2.078 (2) Å, Mg–OH_2 = 2.060 (3) Å)[31] similar to the Mg–O bond distances in **4**.

The hydrogen-bonding network in the lattice of **4**, which is extensive, links the neutral $[Mg_2(EGTA)(OH_2)_6]$ units. It involves all of the water molecules and the "free" oxygen atoms of the carboxylate units bound to Mg^{2+}, in addition to the five occluded water molecules.

Instability of the Magnesium Complex. On the basis of the structure of **4**, one is tempted to conclude that coordination of a Mg^{2+} ion by both of the amino–dicarboxylate termini of the $EGTA^{4-}$ ligand is unlikely in solution, even under conditions of 1/1 $Mg^{2+}/EGTA^{4-}$ stoichiometry. Of course, under such conditions the dinuclear complex **4** cannot be the predominant form in solution; the structure of **4** suggests that in the 1/1 complex the Mg^{2+} ion simply treats $EGTA^{4-}$ as a tridentate iminodiacetate-like ligand. Isolation of **4**, even from solutions of 1/1 $Mg^{2+}/EGTA^{4-}$ stoichiometry (see above), is probably a consequence of the low solubility of this neutral species.

There are, however, other indications that a magnesium ion only binds to one end of the $EGTA^{4-}$ ligand. The equilibrium constants for protonation of a series of ML^{2-} complexes are shown in Table XV. For $ODTA^{4-}$ (H_4ODTA = 3,12-bis(carboxymethyl)-3,12-diazatetradecanedioic acid), the equilibrium constants for protonation of MgL^{2-} and CaL^{2-} are approximately equivalent, and their magnitudes suggest that protonation of amine nitrogen atoms is involved in each case. Given these facts, and the low relative affinities of the metal ions for $ODTA^{4-}$ in comparison to those for $EGTA^{4-}$, it is likely that both Mg^{2+} and Ca^{2+} only bind to one end of $ODTA^{4-}$.

Table XV. Formation and Protonation Constants for Selected Ligands[a]

metal ion	log K			
	EGTA[b]	EEDTA[b]	ODTA[b]	BAPTA[c]
Mg^{2+}	5.2/7.6	8.3/5.0	4.8/9.6	1.8
Ca^{2+}	11.0/3.8	10.0/4.3	4.6/10.0	7.0
Sr^{2+}	8.5/5.3	9.3/4.6	8.7/3.9	
Ba^{2+}	8.4/5.3	8.2/5.2	7.9/4.6	

[a] When two values are given for a metal–ligand combination, the first is log K for $M^{2+} + L^{4-} \rightleftarrows ML^{2-}$, while the second is log K for $ML^{2-} + H^{+} \rightleftarrows HML^{-}$. A single value is log K for the complexation reaction only. [b] Reference 5. [c] Reference 6.

For $EEDTA^{4-}$ (H_4EEDTA = 3,9-bis(carboxymethyl)-6-oxa-3,9-diazaundecanedioic acid), the equilibrium constants for protonation of the Mg^{2+} and Ca^{2+} complexes are also approximately equal but are approximately 5 orders of magnitude less favorable than for $[M(ODTA)]^{2-}$. The $EEDTA^{4-}$ ligand must use both nitrogen atoms to bind Ca^{2+} and Mg^{2+} in order for protonation of these $[M(EEDTA)]^{2-}$ complexes to be so unfavorable. The obvious implication is that $EEDTA^{4-}$ wraps around the calcium and the magnesium ions in the $[M(EEDTA)]^{2-}$ complexes.

For $EGTA^{4-}$, the protonation constant for $[Mg(EGTA)]^{2-}$ is almost 4 orders of magnitude more favorable than for $[Ca(EGTA)]^{2-}$. An obvious explanation for this difference is that one end of the $EGTA^{4-}$ ligand is still free (i.e., uncomplexed) in the 1/1 $Mg^{2+}/EGTA^{4-}$ complex, which leaves one of the amino nitrogen atoms available for relatively favorable protonation. Additionally, the equilibrium constants for formation of the 1/1 Mg^{2+} complexes with $EGTA^{4-}$ and $ODTA^{4-}$ only differ by 0.4 order of magnitude, whereas for the Ca^{2+} complexes, the equilibrium constant for complexation with $EGTA^{4-}$ is over 6 orders of magnitude more favorable than with $ODTA^{4-}$. All of this evidence strongly indicates that a magnesium ion only binds to one end of the $EGTA^{4-}$ ligand in a 1/1 complex, probably in the manner found in **4**.

The $EGTA^{4-}$ analogue $BAPTA^{4-}$ (H_4BAPTA = 1,2-bis(*o*-aminophenoxy)ethane-*N*,*N*,*N*′,*N*′-tetraacetic acid) retains the calcium selectivity characteristic of $EGTA^{4-}$, and the stability of the $[Ca(BAPTA)]^{2-}$ complex does not depend as strongly on pH as does that of the $[Ca(EGTA)]^{2-}$ complex. During spectrophotometric measurement of the formation constants for $BAPTA^{4-}$ complexes, the spectral shift induced by Mg^{2+} was observed to be only half that induced by Ca^{2+}. Much higher concentrations of Mg^{2+} were necessary to produce the spectral shift induced by a given concentration of Ca^{2+}. These results were interpreted as due to sequential binding of two magnesium ions, one at each end of the $BAPTA^{4-}$ ligand.[6] The observation of a dinuclear structure for **4**, with such a similar ligand, adds support to this interpretation.

The inability of $EGTA^{4-}$, and presumably $BAPTA^{4-}$, to chelate Mg^{2+} by using both amino–dicarboxylate termini is probably associated with the high heat of hydration of Mg^{2+} ($\Delta H_{hyd} \approx -460$ kcal mol^{-1} for Mg^{2+} and −375 kcal mol^{-1} for Ca^{2+}).[32-34] Wrapping $EGTA^{4-}$ about a metal ion probably proceeds in a sequential fashion, coordination of one amino–dicarboxylate terminus being followed by coordination of the ether oxygen atoms and finally by coordination of the ligand atoms of the second amino–dicarboxylate terminus. At each step, coordinated water molecules

(27) Metz, B.; Moras, D.; Weiss, R. *Acta Crystallogr., Sect. B: Struct. Crystallogr. Cryst. Chem.* **1973**, *B29*, 1388.
(28) Metz, B.; Moras, D.; Weiss, R. *Acta Crystallogr., Sect. B: Struct. Crystallogr. Cryst. Chem.* **1973**, *B29*, 1382.
(29) Bozhidaev, A. I.; Polynova, T. N.; Porai-Koshits, M. A. *Acta Crystallogr., Sect. A: Cryst. Phys. Diffr., Theor. Gen. Crystallogr.* **1972**, *28*, S76.
(30) Passer, E.; White, J. G.; Cheng, K. L. *Inorg. Chim. Acta* **1977**, *24*, 13.
(31) Stezowski, J. J.; Countryman, R.; Hoard, J. L. *Inorg. Chem.* **1973**, *12*, 1749.
(32) Halliwell, H. F.; Nyburg, S. C. *Trans. Faraday Soc.* **1963**, *59*, 1126.
(33) Benjamin, L.; Gold, V. *Trans. Faraday Soc.* **1954**, *50*, 797.
(34) Ball, M. C.; Norbury, A. H. *Physical Data for Inorganic Chemists*; Longman: London, 1974; p 54.

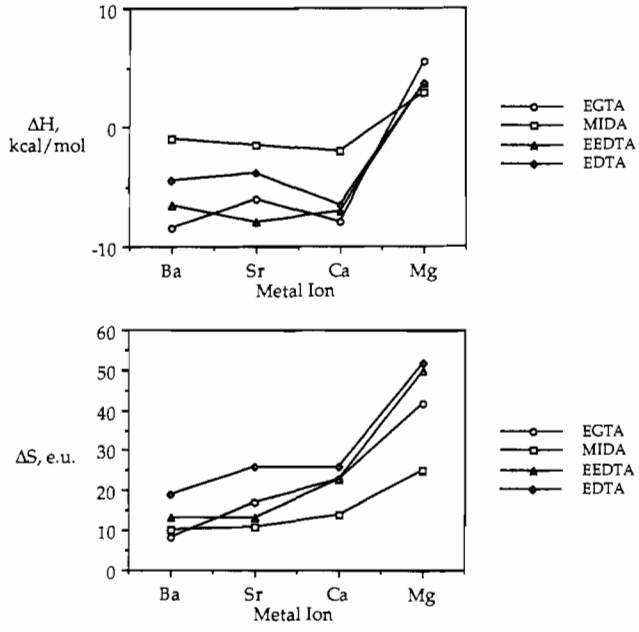

Figure 8. Plots of the enthalpies and entropies of formation for alkaline-earth complexes of $EGTA^{4-}$, $MIDA^{2-}$, $EEDTA^{4-}$, and $EDTA^{4-}$.

must vacate their positions in the coordination sphere. Given the enthalpies above, one can readily appreciate that replacement of coordinated water is energetically much more difficult for Mg^{2+} than for Ca^{2+}. This must mean that while loss of two water molecules to allow replacement by two ether oxygen atoms is relatively easy for Ca^{2+}, the same process is much more energetically costly (by approximately 35 kcal mol^{-1} of water displaced) for Mg^{2+}.

Relative Stabilities of Other Alkaline-Earth–EGTA Complexes. The relative enthalpic and entropic contributions to the stability constants of alkaline-earth–$EGTA^{4-}$ complexes have been measured repeatedly.[9-11] These quantities are depicted in Figure 8 for $EGTA^{4-}$ and the related ligands $EDTA^{4-}$, $MIDA^{2-}$ (H_2MIDA = methyliminodiacetic acid), and $EEDTA^{4-}$.

Formation of the Mg^{2+} complex is entropy-driven for each of the ligands shown in Figure 8 (note the endothermic $\Delta H_f°$ in each case). $EDTA^{4-}$ and $EEDTA^{4-}$ exhibit similar entropic contributions to the stability constants, while $\Delta S_f°$ for the $EGTA^{4-}$ complex is approximately 10 eu less favorable. This less favorable value is consistent with the binding of Mg^{2+} only to one end of the $EGTA^{4-}$ ligand, since tridentate coordination, as seen in **4**, means that fewer water molecules would be released from the $[Mg(OH_2)_6]^{2+}(aq)$ ion on coordination and that the carboxylate groups not involved in coordination to Mg^{2+} would retain solvent ordering properties. However, $EGTA^{4-}$ would also retain some conformational freedom that would be lost upon coordination of both ends of the ligand to a metal ion. The conformational freedom retained in $[Mg(EGTA)]^{2-}$ must be significant, since the entropic contribution to the stability constant is larger for formation of $[Mg(EGTA)]^{2-}$ than for formation of [Mg(MIDA)].

The enthalpic and entropic contributions to the stability constants for Ca^{2+} chelates of $EDTA^{4-}$, $EEDTA^{4-}$, and $EGTA^{4-}$ are nearly identical. The gain in entropy attendant upon displacement of additional water molecules by the chelating ligands with more binding sites must be offset by the loss of entropy attendant upon coordination of a ligand with a greater initial configurational entropy.

The enthalpic and entropic contributions to the stability constants for chelation of the Sr^{2+} and Ba^{2+} ions do not seem to follow a regular pattern. Compared to the Ca^{2+} case, the $\Delta H_f°$ values for $[Sr(EEDTA)]^{2-}$ and $[Ba(EGTA)]^{2-}$ seem to be unusually favorable. It is possible that relief of chelate ring strain by the "planar" coordination of an ether oxygen atom (see above) may play a role in the higher than expected stability of $[Ba(EGTA)]^{2-}$. Structural studies on Ba^{2+} and Sr^{2+} chelates of $EEDTA^{4-}$ would clearly be useful in evaluating this situation.

Inferences for Calcium-Binding Proteins. A magnesium ion is not capable of inducing the protein conformational changes that a calcium ion induces in a calcium-binding protein. A possible reason is that Mg^{2+} may only bind to a subset of the ligand atoms in the highly calcium-selective binding sites in calcium-binding proteins.[35] When $EGTA^{4-}$ binds Mg^{2+}, the metal ion's unwillingness to shed tightly bound water molecules to bind the polydentate ligand's ether oxygen atoms results in binding of the metal to a subset of the available ligand atoms, with a resultant low formation constant. The participation of neutral peptide carbonyl oxygen atoms and hydroxyl groups in calcium binding in the proteins would appear to offer the same sorts of possibilities for discrimination against the Mg^{2+} ion practiced by $EGTA^{4-}$ in this "model" system.

Acknowledgment. The Nicolet R3m/E X-ray diffractometer and computing system at Colorado State University were purchased with funds provided by the National Science Foundation.

Registry No. **1**, 115588-31-3; **2**, 115512-25-9; **3**, 115512-28-2; **4**, 115482-68-3.

Supplementary Material Available: Tables S-I–S-VI, containing respectively the anisotropic thermal parameters, calculated hydrogen atom positions, chelate ring conformational parameters, inter-ring torsion angles, selected least-squares planes, and hydrogen-bonding distances in **1**, Tables S-VIII–S-XIII, containing the corresponding results for **2**, Tables S-XV–S-XX, containing the corresponding results for **3**, and Tables S-XXII–S-XXVI, containing respectively the anisotropic thermal parameters, calculated hydrogen atom positions, chelate ring conformational parameters, selected least-squares planes, and hydrogen-bonding distances for **4** (36 pages); Tables S-VII, S-XIV, S-XXI, and S-XXVII, containing respectively the observed and calculated structure factors (×10) for **1**–**4** (114 pages). Ordering information is given on any current masthead page.

(35) Seamon, K. B.; Kretsinger, R. H. In ref 2a, Chapter 1, p 45.